CRYSTALLIZATION

1. Introduction

Crystallization is one of the oldest unit operations in the portfolio of industrial and/or laboratory separations. Almost all separation techniques involve formation of a second phase from a feed, and processing conditions must be selected that allow relatively easy segregation of the two or more resulting phases. This is also a requirement for crystallization, and there are a variety of other properties of the solid product that must be considered in the design and operation of a crystallizer. Interactions among process, function, product, and phenomena important in crystallization are illustrated in Figure 1.

1.1. Function. Figure 1 lists several possible functions that can be achieved by crystallization: separation, concentration, purification, solidification, and analysis. A few examples follow.

Separation. Sodium carbonate (soda ash) is recovered from a brine by first contacting the brine with carbon dioxide to form sodium bicarbonate. Sodium bicarbonate has a lower solubility than sodium carbonate, and it can be readily crystallized. The primary function of crystallization in this process is separation; a high percentage of sodium bicarbonate is solidified in a form that makes subsequent separation of the crystals from the mother liquor economical. With the available pressure drop across filters that separate liquid and solid, the capacity of the process is determined by the rate at which liquor flows through the filter cake. That rate is set by the crystal size distribution (CSD) produced in the crystallizer.

Separation of a chemical species from a mixture of similar compounds can also be achieved by melt crystallization, which is, eg, an important means of separating *bisphenol A* from the mixture of substances after the reaction. Bisphenol A is crystallized on the inner surface of a tube bundel while the circulated melt flows from top to bottom. On the outside of the tubes, the coolant is flowing also from top to bottom (cocurrent). The crystalline material is recovered

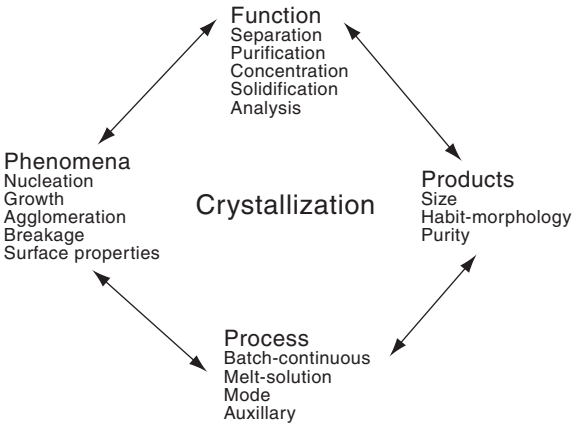

Fig. 1. Crystallization.

by melting. The residue is dischared in liquid form in this batch operation. Very high purities can be achieved if necessary by additional purification steps like sweating or by further crystallization stages with the product of each previous stage until the desired purity is reached. Stripping stages for the required yield are also possible.

Concentration. The concentration of fruit juice requires removal of solvent (water) from the natural juice. This concentration is commonly done by evaporation, but the derived juices may lose flavor components or undergo thermal degradation during evaporation. In freeze concentration, solvent is crystallized (frozen) in a relatively pure form to leave behind a solution with a solute concentration higher than the original mixture. Significant advantages in product taste have been observed in the application of this process to concentration of certain fruit juices.

Purification. The objective of crystallization also can be purification of a chemical species. Well known in examples this respect are sugar and salt. Another example, L-isoleucine (an essential amino acid), is separated by crystallization from a fermentation broth that has been filtered and subjected to ion exchange. The recovered crystals contain impurities deleterious to use of the product, and these crystals are, therefore, redissolved and recrystallized to enhance purity.

Solidification. Production of a product in a form suitable for use and acceptable to the consumer also may be an objective of a crystallization process. For example, the appearance of sucrose (sugar) varies with local customs, and deviations from that custom could lead to an unacceptable product. A final crystallization may thus be called for to bring the product appearance into compliance with expectations. Another example is liquid sulfur that has to be solidified and is liquid sulfur that is solidified as pastilles to provide for a free flowing, dust free product.

Analysis. Many analytical procedures calling for determination of molecular structure are aided by crystallization or require that the unknown compound be crystalline. Methodologies coupling crystallization and analytical procedures will not be covered here (see X-RAY DIFRACTION).

1.2. Products. In all of the instances in which crystallization is used to carry out a specific function, product requirements are a central component in determining the ultimate success of the process. These result as a consequence of how the product is to be used and the processing steps between crystallization and recovery of the final product. Key determinants of product quality are the size distribution (including crystal mean size and variance), the morphology (including habit or shape and form), and purity. Of these, only the last is important with other separation processes.

Crystal size distribution, including the problem of fines (dust), determines several important processing and product properties, including crystal appearance, separation of crystals from the liquor, reactions, dissolution, and other processes and properties involving the surface area of the crystalline product, crystal transportation, and crystal storage. In fact, experience indicates that a large fraction of crystallizer troubleshooting cases have been initiated to solve problems associated with inadequate throughput of filters or centrifuges; when solutions are found they generally involve manipulation of CSD.

It is often important to control the CSD of pharmaceutical compounds, eg, in the synthesis of human insulin, which is made by recombinant DNA techniques (1). The most favored size distribution is one that is monodisperse, ie, all crystals are of the same size, so that the rate at which the crystals dissolve and are taken up by the body is known and reproducible. Such uniformity can be achieved by screening or otherwise separating the desired size from a broader distribution or by devising a crystallization process that will produce insulin in the desired form. The latter of these options is preferable, and considerable effort has been expended in that regard.

1.3. Process. In each of the systems discussed above there is a need to form crystals, to cause the crystals to grow, and to separate the crystals from residual liquid. There are various ways to accomplish these objectives leading to a multitude of processes, batch or continuous, that are designed to meet requirements of product yield, purity, and, uniquely, CSD.

1.4. Phenomena. The critical phenomena in crystallization are, as shown in Figure 1, generation of supersaturation, nucleation and growth kinetics, interfacial phenomena, breakage, and agglomeration. Nucleation leads to the formation of crystals, either from a solution or a melt. Growth is the enlargement of crystals caused by deposition of solid material on an existing surface. The relative rates at which nucleation and growth occur determine the CSD qualitatively, when the rate of nucleation is high relative to growth rate, crystals formed are small and numerous. Agglomeration is the formation of a larger particle through two or more smaller particles (crystals) sticking together. It is prevalent in many processes, and agglomeration can be essential for solid–liquid separation or it can be undesirable because it may adversely affect crystal quality. Breakage of crystals is almost always undesirable because it is detrimental to crystal appearance and it can lead to excessive fines and have a deleterious effect on crystal purity. Interfacial phenomena influence solid–liquid separation, flow characteristics of slurries, agglomeration, and crystal morphology.

2. Solid–Liquid Equilibria and Mass and Energy Balances

2.1. Solubility. Solid–liquid equilibrium, or the solubility of a chemical compound in a solvent, refers to the amount of solute that can be dissolved at constant temperature, pressure, and system composition; in other words, the maximum concentration of the solute in the solvent at static conditions. In a system consisting of a solute and a solvent, specifying system temperature and pressure fixes all other intensive variables. In particular, the composition of each of the two phases is fixed, and solubility diagrams of the type shown for a hypothetical mixture of R and S in Figure 2 can be constructed. Such a system is said to form an eutectic, ie, there is a condition at which both R and S crystallize into a solid phase at a fixed ratio that is identical to their ratio in solution. Consequently, there is no change in the composition of residual liquor as a result of crystallization.

Several features of the hypothetical system in Figure 2 can be used to illustrate proper selection of crystallizer operating conditions and limitations placed on the operation by system properties. Suppose a saturated solution at

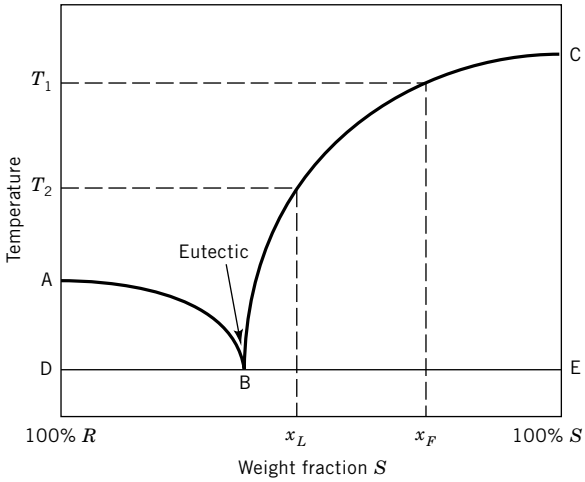

Fig. 2. Solubility diagram for a hypothetical system. The curves AB and BC represent solution compositions that are in equilibrium with solids whose compositions are given by the lines AD and CE. If AD and CE are vertical along the respective axes, the crystals are pure R and S, respectively. Crystallization from any solution whose composition is to the left of the vertical line through point B produces crystals of pure R, whereas solutions to the right of the line produce crystals of pure S. A solution whose composition falls on the line through B produces a solid mixture that has a composition identical to the liquid solution.

temperature T_1 is fed to a crystallizer operating at temperature T_2. Because the feed is saturated, the weight fraction of S in the feed is given as shown in Figure 2. The maximum crystal production rate $P_{\max}$ from such a process depends on the value of T_2 and is given by

$$P_{\max} = F_{\chi F} - L_{\chi \mathrm{L}} \tag{1}$$

where F is the feed rate to the crystallizer, and L is the solution flow rate leaving the crystallizer. No other stream is fed to or removed from the crystallizer. Note that the lower limit on T_2 is given by the eutectic point B.

Figure 3 presents the equilibrium behavior of magnesium sulfate in water, and it is illustrative of systems that form hydrated salts. Equilibrium solution concentrations are plotted as curves *ab*, *bc*, *cd*, *de*, and *ef*; the solid phases that are in equilibrium with these solutions have compositions given by the lines ag, hi, *jk*, lm, and *no*, respectively. Ice is the solid phase whose composition is given by *ag*, and crystals containing differing ratios of water of hydration to magnesium sulfate constitute the solids represented by the other lines. Specifically, the line *no* represents magnesium sulfate monohydrate ($MgSO_4 \cdot H_2O$), which has one water molecule per molecule of magnesium sulfate, whereas the lines *ml*, *kj*, and *ih* represent the hexahydrate, heptahydrate, and dodecahydrate forms, respectively. The weight fraction of $MgSO_4$ in each of the crystal forms is shown in Figure 3, and as with all crystalline materials having water of hydration, the solute balance of equation 1 must be modified to read

$$\chi_c P_{\max} = F_{\chi_F} - L_{\chi_L} \tag{2}$$

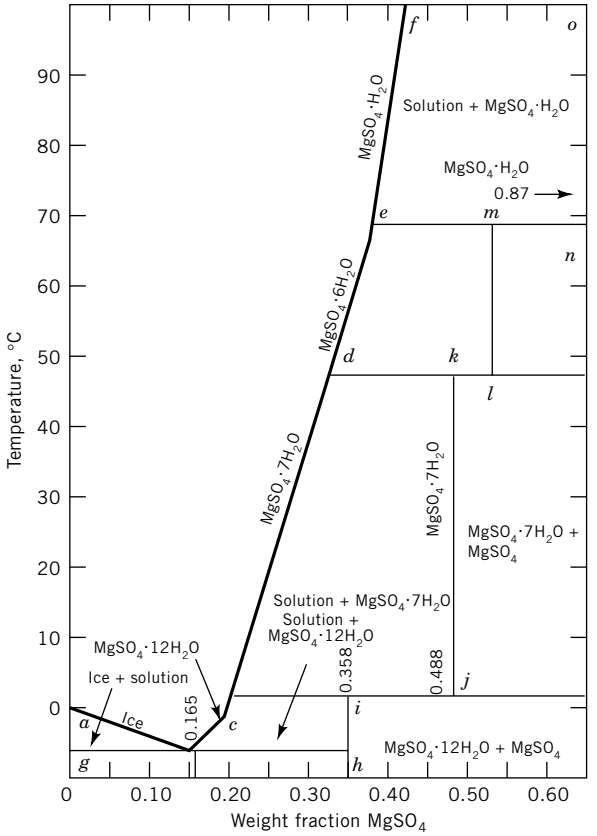

Fig. 3. Solubility diagram for magnesium sulfate in water (2,3).

where x_c is the mass fraction of solute in the crystal, eg, x_c is 0.488 when the crystalline substance is magnesium sulfate heptahydrate. Differences in the forms of magnesium sulfate crystals affect the dependence of solubility on temperature, which is reflected by the slopes of the solution composition curves.

A solubility curve, as found in Figure 4, is just a small window of the phase diagram as, eg, seen in Figure 2. This is immediately clear after exchanging the axes. By discussing solutions and melts, we reflect on the historical developments in the crystallization of different materials rather than their different physical phenomena.

The dependence of solubility on temperature affects the mode of crystallization. For example, Figure 4 shows that the solubility of potassium nitrate (KNO_3) is strongly influenced by the system temperature but that temperature has little influence on the solubility of sodium chloride (NaCl). As a consequence, a reasonable yield of KNO_3 crystals can be obtained by cooling a saturated feed solution; on the other hand, cooling a saturated sodium chloride solution accomplishes little crystallization, and evaporation is required to increase the yield of sodium chloride crystals.

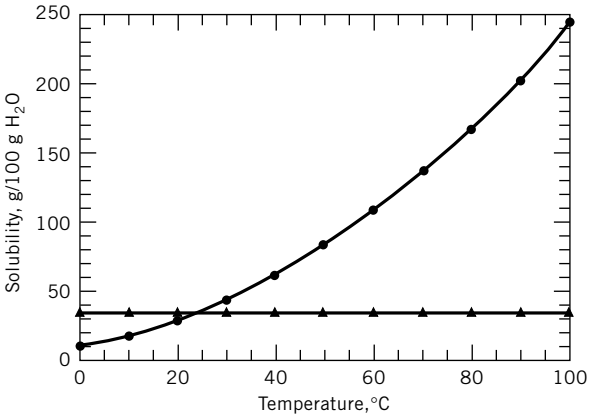

Fig. 4. Solubilities of NaCl ▲, and KNO_3 ●, in H_2O (2,3).

The production of many high value chemicals requires maximizing separation from a relatively dilute solution. It is common in such instances to use a combination of methods to reduce solute solubility in the feed solution. Figure 5, eg, illustrates that the addition of methanol to a saturated aqueous solution of L-serine can reduce solubility by more than an order of magnitude.

Solubility data can be found in a variety of units, and conversion from one set of units to another often is required before computation of yield can be performed. Guides to such conversions are available. It is often most convenient, however, to express solubility and compositions in mixed streams in terms of mass ratios, ie, mass of solute per mass of solvent.

2.2. Supersaturation. The thermodynamic driving force for both crystal nucleation and growth is the key variable in setting the mechanisms and rates by which these processes occur. Supersaturation is defined rigorously as the

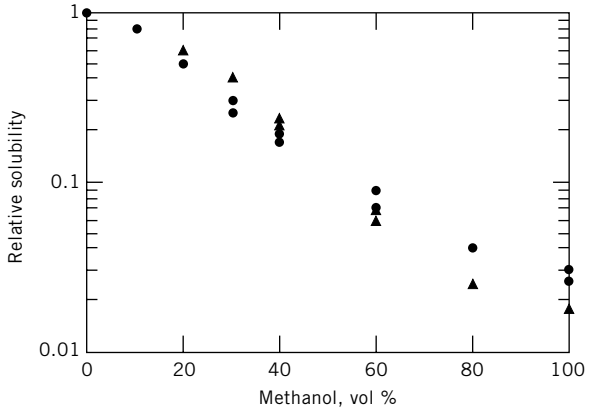

Fig. 5. Solubilities of L-serine in mixtures of methanol (CH_3OH) and water (H_2O). Relative solubility = solubility in $CH_3OH - H_2O \div$ solubility in H_2O; ■, 10°C: ▲, 30°C. Reproduced by permission of the American Institute of Chemical Engineers (4).

deviation from thermodynamic equilibrium, which is the difference between the chemical potential of the solute in solution μ and the chemical potential of the solution in equilibrium with the solid phase μ^*. Less abstract definitions involving measurable system properties such as temperature, concentration, or mass or mole fraction also have been used to express supersaturation. Consider, eg, a system at temperature T with a solute concentration c. A saturated solution having a concentration c would be at temperature T^*, whereas a saturated solution having a temperature T would have a solute concentration c^*.

Expressions of supersaturation can then be formulated as follows: (*1*) the difference between the chemical potential of the system and the chemical potential of saturation, $\mu - \mu^*$, where the chemical potential is a function of both temperature and concentration; (*2*) the difference between the solute concentration and the concentration at equilibrium, $c - c^*$; (*3*) the difference between the system temperature at equilibrium and the actual temperature, $T^* - T$; (*4*) the ratio of the solute concentration and the equilibrium concentration, c/c^*, which is known as relative saturation; or (*5*) the ratio of the difference between the solute concentration and the equilibrium concentration to the equilibrium concentration, $s = (c - c^*)/c^*$, which is also known as relative supersaturation. This term has often been represented by σ; s is used here because of the frequent use of σ for interfacial energy or surface tension and for variance in distribution functions.

Any of these definitions of supersaturation can be used over a moderate range of system conditions. For example, a difference in chemical potential $\Delta\mu = \mu - \mu^*$ is proportional to both $c - c^*$ and $T^* - T$ over a modest range of conditions. Of the five expressions given, however, the second is most useful in calculating the yield from a crystallizer, the third provides information that may be most useful in the control of a crystallizer, and the fifth is most commonly used in correlating the dependence of nucleation and growth kinetics on supersaturation.

Although the first of these expressions is the most nearly fundamentally correct, it is difficult to evaluate because of inadequate capabilities of determining chemical potential as a function of temperature and composition. The most useful driving force expression for crystal growth is that given by the last of the possibilities, ie, $s = (c - c^*)/c^*$. This definition of supersaturation will be used throughout the ensuing discussion, but it should be recognized that the validity of doing so is limited to low supersaturations. Solute concentrations used in determining supersaturation should include any water of hydration associated with the solute in the crystal at equilibrium. In the case of melts definition (3) $T^* - T$ is the most commonly used.

2.3. Mass and Energy Balances. The formulation of mass and energy balances follows procedures outlined in many basic texts (2). The use of solubilities to calculate crystal production rates from a cooling crystallizer is given by equations 1 and 2. Subsequent to determining the yield, the rate at which heat must be removed from such a crystallizer can be calculated from an energy balance:

$$F\hat{H}_F = P\hat{H}_C + L\hat{H}_L + Q \tag{3}$$

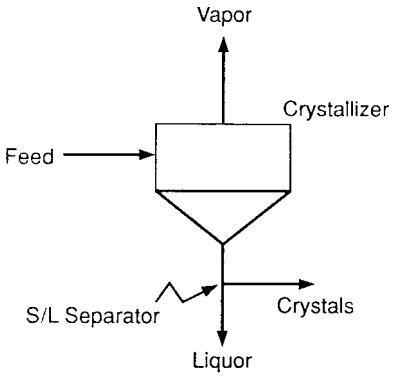

Fig. 6. Schematic diagram of a simple crystallizer.

where F, P, and L are feed rate, crystal production rate, and mother liquor flow rate, respectively; $\hat{H}$ is the specific enthalpy of the stream corresponding to the subscript; and Q is the required rate of heat transfer. As F, P, and L are known or can be calculated from a simple mass balance, determination of Q requires methods of estimating specific enthalpies.

If appropriate enthalpy data are unavailable, estimates (with such assumptions as constant heat capacities in the temperature range considered) can be obtained by first defining reference states for both solute and solvent. Often the most convenient reference states are crystalline solute and pure solvent at an arbitrarily chosen reference temperature. The reference temperature selected usually corresponds to that at which the heat of crystallization $\Delta\hat{H}_c$ of the solute is known. The heat of crystallization is approximately equal to the negative of the heat of solution. For example, if the heat of crystallization is known at T_{ref}, then reasonable reference conditions would be the solute as a solid and the solvent as a liquid, both at T_{ref}. The specific enthalpies then could be evaluated as

$$\hat{H}_F = \chi_F \Delta_C + C_{\text{pF}}(T - T_{\text{ref}}) \tag{4}$$

$$\hat{H}_C = C_{\text{pC}}(T - T_{\text{ref}}) \tag{5}$$

$$\hat{H}_L = \chi_L \Delta\hat{H}_C + C_{\text{pL}}(T - T_{\text{ref}}) \tag{6}$$

where χ_F and χ_L are the mass fractions of solute in the feed and mother liquor, respectively. All that is required now to determine the required rate of heat transfer is the indicated heat capacities, that can be estimated or measured experimentally.

Now, suppose some of the solvent is evaporated in the crystallizer, as is shown in Figure 6. Independent balances can be written on total mass and solute:

$$F = V + L + P \tag{7}$$

$$\chi_F F = \chi_L L + \chi_C P \tag{8}$$

where F = feed rate, V = vapor withdrawal rate, L = liquid (filtrate) withdrawal rate, and P = crystal production rate, and χ_j = solute content of stream j in units consistent with flow rate. There is an equilibrium expression relating χ_L, χ_C, and the temperature or pressure at which the operation is conducted. In addition, an energy balance must be satisfied

$$F\hat{H}_F + Q = V\hat{H}_V + L\hat{H}_L + P\hat{H}_C \tag{9}$$

The specific enthalpies ($\hat{H}_j$) in equation 9 can be determined as described earlier, provided the temperatures of the product streams are known. Evaporative cooling crystallizers operate at reduced pressure and may be considered adiabatic ($Q = 0$). As with many problems involving equilibrium relationships and mass and energy balances, trial-and-error computations are often involved in solving equations 7–9.

The mass balance on a crystallizer is related to the growth kinetics occurring within the unit. This may be simplified by considering systems in which crystal growth kinetics are sufficiently fast to depelete essentially all of the supersaturation provided by the crystallizer. Under such conditions (referred to in the crystallization literature as class II or fast-growth behavior), the solute concentration in the mother liquor can be assigned a value corresponding to saturation. Alternatively, should supersaturation in the mother liquor be so great as to affect the solute balance, the operation is said to follow class I or slow-growth behavior. An expression coupling the rate of growth to a solute balance must be used to describe such a system.

3. Crystallization Kinetics

Along with operating variables of the crystallizer, nucleation and growth kinetics determine such crystal characteristics as size distribution, purity, and shape or habit.

3.1. Nucleation. Crystal nucleation (5) is the formation of an ordered solid phase from a liquid or amorphous phase. Nucleation sets the character of the crystallization process, and it is, therefore, the most critical component in relating crystallizer design and operation to CSD.

Mechanisms. Classical nucleation theory is based on homogeneous and heterogeneous mechanisms, both of which involve the formation of crystals through a process of combining the constituent units (atoms, ions, or molecules) that form a crystal sequentially. Heterogeneous and homogeneous mechanisms are referred to as primary nucleation because existing crystals play no role in the nucleation. Primary nucleation can be illustrated by considering a hypothetical experiment in the context of the solubility data in Figure 7. Assume that a solution is at a concentration and temperature corresponding to point A on the figure. The solution is undersaturated, so any crystals present in the system would dissolve. If the concentration is increased at constant temperature, eg by evaporation, the path followed would cause the solution to reach saturated conditions at point B. Once the concentration becomes greater than that at B, the solution is supersaturated and any crystals present in the system would grow.

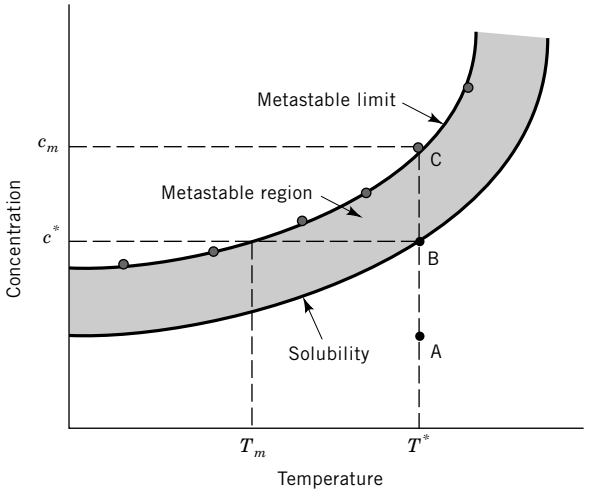

Fig. 7. Solubility and primary nucleation in a hypothetical experiment.

However, experience shows that nucleation would not occur until the concentration reaches point C, which defines what is called the metastable limit. If this procedure is repeated at various temperatures, a metastable limit curve could be drawn as shown.

Primary nucleation will not occur, within the metastable region, and the width of the metastable zone, as reflected by $c_m - c^*$ or $T^* - T_m$, varies from one substance to another. Furthermore, the width can vary for the same substance with temperature, composition, the presence of impurities (6) that alter interfacial tension, and various other factors.

In contrast to the thermodynamically defined solubility curve, the metastable limit curve is not thermodynamically defined and is strongly dependent on process parameters such as temperature level, rate of supersaturation change, degree of agitation.

Both homogeneous and heterogeneous mechanisms require relatively high supersaturation, and exhibit a high order dependence on supersaturation. These factors often lead to production of excessive fines in systems where primary nucleation mechanisms are important. The classical theoretical treatment of primary nucleation results for spherically shaped nuclei in the expression (7)

$$B^0 = A \exp\left(-\frac{16\pi\sigma^3\nu^2}{3k^3T^3[\ln(s+1)]^2}\right) \tag{10}$$

where B^0 is the nucleation rate at zero size, k is the Boltzmann constant, σ is surface energy per unit area, ν is molar volume, and A is a constant. This equation can be simplified by recognizing that $\ln(s+1)$ approaches s as s approaches 0. So for small supersaturations,

$$B^0 = A \exp\left(-\frac{16\pi\sigma^3\nu^2}{3k^3T^3s^2}\right) \tag{11}$$

The most important variables affecting nucleation rate are shown by equations 10 and 11 to be interfacial energy, temperature, and supersaturation.

The high order dependence of nucleation rate on supersaturation is especially important because a small swing in supersaturation may produce an enormous change in nucleation rate. This gives rise to the often-observed phenomenon of having a clear liquor transformed into a slurry of fine crystals with only a slight increase in supersaturation, eg, by decreasing the solution temperature.

The catalytic effect of solid surfaces (as in heterogeneous nucleation) is to reduce the energy barrier to formation of a new phase, which in effect, can reduce the interfacial energy σ significantly.

The metastable limit can provide an empirical approach to modeling primary nucleation. This limit, which was first observed in 1951 (8), must be determined through experimentation. Nucleation rate can be correlated with the following equation:

$$B^0 = k(c^* - c_m)^i \tag{12}$$

where the equilibrium concentration c^* is less than the concentration at the metastable limit, c_m. Values of c_m are often very close to c^* for many inorganic systems, and satisfactory correlations have been obtained with c^* substituted for c_m in equation 12 (9); in other words,

$$B^0 = k(c - c^*)^i \tag{13}$$

where the parameters k and i must be evaluated from experimental data.

Secondary nucleation is crystal formation through a mechanism involving the solute crystals; crystals of the solute must be present for secondary nucleation to occur. Thorough reviews of secondary nucleation have been published (10,11).Several features of secondary nucleation make it more important than primary nucleation in industrial crystallizers. First, continuous crystallizers and seeded batch crystallizers have crystals in the magma that can participate in secondary nucleation mechanisms. Second, the requirements for the mechanisms of secondary nucleation to be operative are fulfilled easily in most industrial crystallizers. Finally, low supersaturation can support secondary but not primary nucleation, and most crystallizers are operated in a low supersaturation regime that improves yield and enhances product purity and crystal morphology.

Secondary nucleation can occur as the result of several mechanisms that have been identified in selected systems and include the following. *Initial breeding* results from immersion of seed crystals in a supersaturated solution. It is thought to be caused by dislodging extremely small crystals that were formed on the surface of larger crystals during drying. Although this mechanism is unimportant in continuous and unseeded batch crystallization, it can be significant in the operation of seeded batch crystallizers. Several process variables have been shown to influence nucleation rates caused by initial breeding (12). *Contact nucleation* results from collisions of crystals with one another, and/or crystallizer internals, and/or an impeller in an agitator or circulation pump. The collision

energy required for contact nucleation is small and does not result in macroscopic degradation (breakage) of the contacted crystal (13). *Shear breeding* results when supersaturated solution flows by a crystal surface and carries with it crystal precursors formed in the region of the growing crystal surface. In a study of nucleation of $MgSO_4 \cdot 7H_2O$ by this mechanism, it was found (14) that high levels of supersaturation were required for it to produce significant numbers of nuclei.

Process Variables Affecting Contact Nucleation. Pioneering studies elucidated many factors affecting contact nucleation (15–18). The number of crystals produced by a controlled impact of an object with a seed crystal depends on energy of impact, supersaturation at impact, supersaturation at which crystals mature, hardness of the impacting object (19–21), area of impact, angle of impact, and system temperature. Although it is impossible to account quantitatively for all of these variables, certain generalizations can be drawn from the research on this nucleation mechanism.

Based on experimental observations, the following expression was proposed (22) for systems at constant supersaturation:

$$B^0 = k_N \exp(E - E_t) \tag{14}$$

The same researchers proposed that a relationship of impact energy E to crystallizer variables must include the mass of the impacting crystal m_c, the rotational velocity of the impeller providing mixing ω, and the fraction of the available energy actually transmitted to the crystal ϵ:

$$E = f(\omega, \epsilon, m_c) \tag{15}$$

Correlations of nucleation rates with crystallizer variables have been developed for a variety of systems. Although the correlations are empirical, a mechanistic hypothesis regarding nucleation can be helpful in selecting operating variables for inclusion in the model. Two examples are (*1*) the effect of slurry circulation rate on nucleation has been used to develop a correlation for nucleation rate based on the tip speed of the impeller (9,23) and (*2*) the scaleup of nucleation kinetics for sodium chloride crystallization provided an analysis of the role of mixing and mixer characteristics in contact nucleation (24). Published kinetic correlations have been reviewed through ~1979 (25). In a later section on population balances, simple power-law expressions are used to correlate nucleation rate data and describe the effect of nucleation on crystal size distribution.

Supersaturation has been observed to affect contact nucleation (26), but the mechanism by which this occurs is not clear. There are data (27) that infer a direct relationship between contact nucleation and crystal growth. This relationship has been explained by showing that the effect of supersaturation on contact nucleation must consider the reduction in interfacial supersaturation due to the resistance to diffusion or convective mass transfer (28).

Still another possible role of supersaturation is that it affects the solution structure and causes the formation of clusters of solute molecules. These clusters may participate in nucleation, although the mechanism by which this would occur is not clear. Evidence of the existence of cluster formation in

supersaturated solutions has been presented for citric acid (29); while others have examined the phenomenon in greater detail (30,31).

The ease with which nuclei can be produced by contact nucleation is a clear indication that this mechanism is dominant in many industrial operations. Research on contact nucleation is continuing with the objective of building an understanding of the phenomenon that will allow its successful inclusion in models describing commercial systems (32–34).

3.2. Crystal Growth. In most of the literature and in textbooks the model of two resistance's determining growth kinetics is promoted: (*1*) those associated with integration or incorporation of the crystalline unit (eg, solute molecules) into the crystal surface (lattice) and (*2*) molecular or bulk transport of the unit from the surrounding solution to the crystal face. However, it has been proven that the heat resistance is also of equal importance (35–37). This is especially important for melts and can in most cases be reduced to the a. m. two resistance's in the case of solution crystallization. The primary concern here is with surface incorporation. A simple set of experiments in which the rate of advance of a crystal face is measured can be used to illustrate these two resistance's. Data given in Figure 8 show the effect of solution velocity over a crystal face at three different conditions. As the solution velocity increases from low values, the growth rates also increase. At ~24 cm/s, however, the growth rates approach constant values. Such behavior indicates that both bulk mass transfer and surface incorporation are important <24 cm/s but above this velocity, surface incorporation provides the dominant resistance to growth.

Growth Models. Numerous models have been proposed to describe surface reaction kinetics, including those that assume crystals grow by layers and others that consider growth to occur by the movement of a continuous step. Each model results in a specific relationship between growth rate and supersaturation, but none can be used for a priori predictions of growth kinetics. Insights regarding the roles of certain process variables can be obtained, however, and with additional research, predictive capabilities may be achieved. For these reasons and because of extensive literature on the subject (7,38–46), all that will be

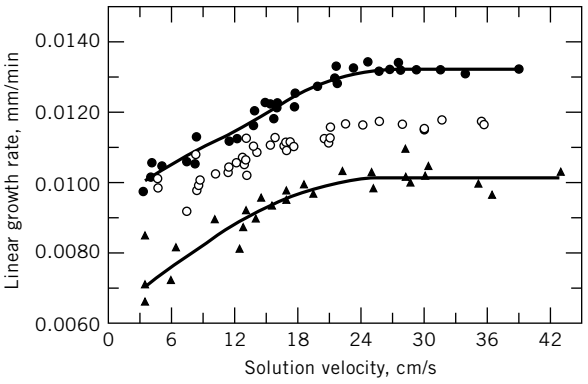

Fig. 8. Effect of solution velocity on the growth rate of the <110> face of $MgSO_4 \cdot 7H_2O$. Concentration of $MgSO_4$: ■; 29.02 % wt % at 30.8°C; o, 28.89 wt % at 30.8°C; ▲, 18.89 wt % at 31.3°C.

pointed out here are the key aspects of the physical models and the resulting relationship between growth and supersaturation predicted by each theory.

Models used to describe the growth of crystals by layers call for a two-step process: (*1*) formation of a two-dimensional (2D) nucleus on the surface and (*2*) spreading of the solute from the 2D nucleus across the surface. The relative rates at which these two steps occur give rise to the mononuclear 2D nucleation theory and the polynuclear 2D nucleation theory. In the mononuclear 2D nucleation theory, the surface nucleation step occurs at a finite rate, whereas the spreading across the surface is assumed to occur at an infinite rate. The reverse is true for the polynuclear 2D nucleation theory. From the mononuclear 2D nucleation theory, growth is related to supersaturation by equation 16.

$$G = C_1 hA[\ln(1+s)]^{1/2} \exp\left[-\frac{C_2}{T^2 \ln(1+s)}\right] \tag{16}$$

where C_1 and C_2 are system-dependent constants, h is the height of the nucleus, A is surface area, and s and T are as defined earlier. The polynuclear 2D theory produces equation 17.

$$G = \left(\frac{C_3}{T^2[\ln(1+s)]^{3/2}}\right) \exp\left[-\frac{C_2}{T^2 \ln(1+s)}\right] \tag{17}$$

where C_3 is a system-dependent constant. Finally, if both formation of the 2D nucleus and spreading of the surface layer are important in determining growth rate, the equation 18 can be derived

$$G = C_4 s^{2/3} [\ln(1+s)]^{1/6} \exp\left[-\frac{C_2}{3T^2 \ln(1+s)}\right] \tag{18}$$

where C_4 is a system-dependent constant.

Equations 16–18 can be simplified considerably by recognizing that in many systems the quantity s is much $\ll 1$. In that case, $\ln(1+s)$ is approximately equal to s. By making this substitution, the growth rate from the mononuclear 2D nucleation theory becomes

$$G = C_1 hA s^{1/2} \exp\left(-\frac{C_2}{T^2 s}\right) \tag{19}$$

For the polynuclear 2D nucleation theory

$$G = \left(\frac{C_3}{T^2 s^{3/2}}\right) \exp\left(-\frac{C_2}{T^2 s}\right) \tag{20}$$

For both steps occurring at similar rates

$$G = C_4 s^{5/6} \exp\left(-\frac{C_2}{T^2 s}\right) \tag{21}$$

The screw dislocation theory (41) , often referred to as the BCF theory (after its formulators Burton, Cabrera, Frank), shows that the dependence of growth rate on supersaturation can vary from a quadratic relationship at low supersaturation to a linear relationship at high supersaturation. In the BCF theory, growth rate is given by

$$G = C\left(\frac{\epsilon s^2}{\sigma'_1}\right)\tanh\left(\frac{\sigma'_1}{\epsilon s}\right) \tag{22}$$

where ε is screw dislocation activity and σ'_1, is a system-dependent quantity that is inversely proportional to temperature. The dependence of growth rate on supersaturation is linear if the ratio $\sigma_1 / \varepsilon s$ large, but the functional dependence becomes parabolic as the ratio becomes small. This is because $(\frac{\sigma'_1}{\epsilon s}) \longrightarrow \frac{\sigma'_1}{\epsilon s}$ as $\frac{\sigma'_1}{\epsilon s}$ becomes small (supersaturation becomes large), and $(\frac{\sigma'_1}{\epsilon s}) \longrightarrow 1.0$ as $\frac{\sigma'_1}{\epsilon s}$ becomes large (supersaturation becomes small). It is thus possible to observe variations in the dependence of growth rate on supersaturation for a given crystal–solvent system.

An empirical approach can also be used to relate growth kinetics to supersaturation with a power-law function of the form

$$G = k_{\mathrm{G}} s^g \tag{23}$$

where k_{G} and g are constants determined by fitting the equation to growth-rate data. Such an approach should be valid over small ranges of supersaturation, and analysis of the theories discussed above shows that the more fundamental equations can be fit by equation 23 over limited ranges of supersaturation. For example, using the empirical approach to describe systems in which the screw dislocation model was applicable would limit g to values between 1 and 2, assuming ϵ was independent of supersaturation.

All the models described above indicate the importance of system temperature on growth rate. Dependencies of growth kinetics on temperature are often expressed in terms of an Arrhenius expression:

$$k_G = k_G^0 \exp\left(-\frac{\Delta E_G}{RT}\right) \tag{24}$$

where k_G is a growth rate coefficient of the type required in equation 23, $K_G{}^0$ is a constant, and ΔE_G is an activation energy. The magnitude of ΔE_G can be as large as that for many chemical reactions, 42 kJ/mol (>10 kcal/mol).

Both supersaturation and temperature can have different effects on the growth rates of different faces of the same crystal. Such occurrences have implications with respect to crystal habit, and these are dealt with in a later section.

Effects of Impurities and Solvent. The presence of impurities usually decreases the growth rates of crystalline materials, and problems associated with the production of crystals smaller than desired are commonly attributed to contamination of feed solutions. Strict protocols should be followed in operating units upstream from a crystallizer to minimize the possibility of such occurrences. Equally important is monitoring the composition of recycle streams

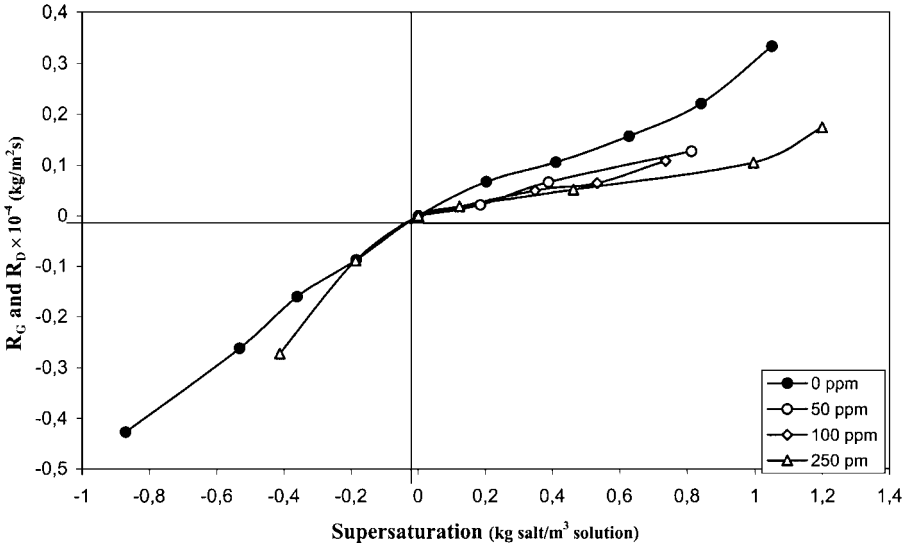

Fig. 9. Growth and dissolution rates of NaCl in the presence of $MgCl_2$ [(of different amounts (0–250 ppm)] after correction of the saturation (kinetic effect) (47).

to prevent possible accumulation of impurities. Furthermore, crystallization kinetics used in scaleup should be obtained from experiments on solutions as similar as possible to those expected in the full-scale process.

Figures 9 and 10 (47) show that $MgCl_2$ reduces the growth rate of NaCl. The reduction is stronger with increasing amounts of $MgCl_2$ (see Fig. 9 the kinetic effect). This is, however, only clear after a correction in the saturation point.

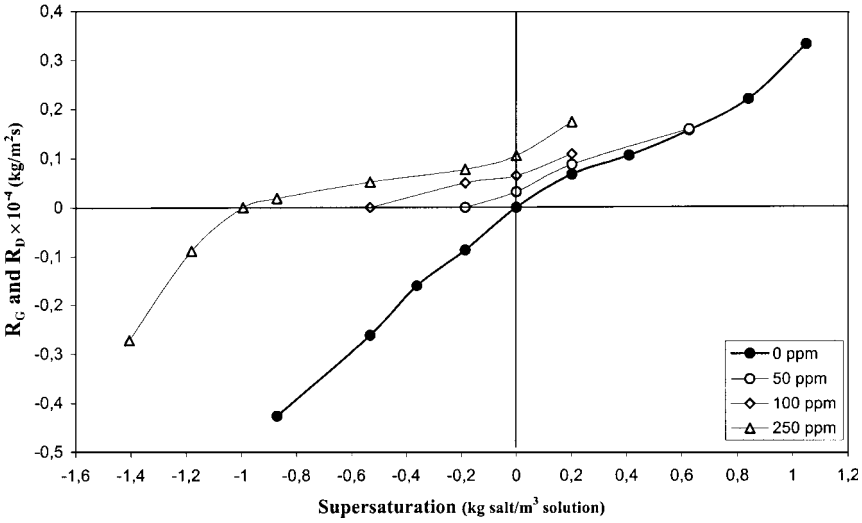

Fig. 10. Growth and dissolution rates of NaCl in the presence of $MgCl_2$ of different amounts (0–250 ppm) (thermodynamic effect) (47).

Figure 10 gives the same data as in Figure 9 taken from the experiments before the correction. An increase in growth rate of NaCl seems to be suggested with an increase in $MgCl_2$, however, this is only a shift in the saturation point, the thermodynamic effect.

The effects of a solvent on growth rates have been attributed to two phenomena (42): one has to do with the effects of solvent on mass transfer of the solute through changes in viscosity, density, and diffusivity; the second is concerned with the structure of the interface between crystal and solvent. The analysis (42) concludes that a solute–solvent (there are also molecular interactions between solute and solvent) system that has a high solubility is likely to produce a rough interface and, concomitantly, large crystal growth rates.

Crystal Growth in Mixed Crystallizers. Multicrystal magma studies usually involve examination of the rate of change of a characteristic crystal dimension or the rate of increase in the mass of crystals. The characteristic dimension depends on the method used in the determination of size; eg, the second-largest dimension is measured by sieve analyses, whereas electronic-zone-sensing instruments provide estimates of an equivalent spherical diameter, and laser-light-scattering gives a dimension close to the largest dimension of a particle, if it is randomly oriented relative to the laser beam path. If the rate of change of a crystal mass dM_c/dt is measured, the quantity can be related to the rate of change in the crystal characteristic dimension by the equation

$$\frac{dM_c}{dt} = \frac{d\left(\rho_c k_v L^3\right)}{dt} = 3\rho_c k_v L^2 \frac{dL}{dt} \tag{25}$$

where ρ_c is crystal density and k_v is the volume shape factor. Because an area shape factor can be defined by the equation

$$k_a = A_c/L^2 \tag{26}$$

where A_C is the crystal surface area and G is defined as dL/dt,

$$\frac{dM_c}{dt} = 3\rho_c \left(\frac{k_v}{k_a}\right) A_c G \tag{27}$$

The formulation of a population balance requires defining growth rate as the rate of change of the characteristic dimension

$$G = \frac{dL}{dt} \tag{28}$$

and solution of the resulting differential population balance requires a knowledge of the relationship between growth rate and size of the growing crystals. Moreover, this relationship can often be deduced from the form of population density data. A special condition, which simplifies such balances, results when all crystals in the magma grow at a rate independent of crystal size. Crystal–solvent systems that show this behavior are said to follow the ΔL law (43) whereas systems that do not are said to exhibit anomalous growth.

Anomalous growth means that growth rates of crystals in a magma are not identical or that the growth rate of an individual crystal or mass of crystals is not constant. Two theories have been used to explain growth rate anomalies: size-dependent growth and growth rate dispersion. Both alter the form of the population density function obtained from perfectly mixed continuous crystallizers; unfortunately, such behavior cannot be used to distinguish between size-dependent growth and growth rate dispersion, as both have the same qualitative effects on population density.

3.3. Size-Dependent Crystal Growth. A number of empirical expressions correlate the apparent effect of crystal size on growth rate (48). The most commonly used correlation uses three empirical parameters to correlate growth rate with crystal size:

$$G = G^0(1 + \gamma L)^b \qquad b < 1 \tag{29}$$

where G^0, γ, and b are determined from experimental data. There have been attempts to relate the kinetic parameter b to crystallizer variables. The only success in this regard (49) showed a qualitative dependence on crystallizer volume. Several theories have been proposed to explain size-dependent growth kinetics, but none has been substantiated by direct observation or used to predict the onset of such behavior. One explanation seems particularly appealing: larger crystals impact impellers and other crystallizer internals with higher frequency and energy than smaller crystals; therefore, the larger crystals are recipients of more surface breaks and irregularities that lead to higher growth rates. Furthermore, it is true that larger crystals have a higher thermal velocity and therefore a thinner concentration boundary layer and allow therefore a faster mass transfer. The conclusion is that there is no size-dependent growth, however, the use of such a model leads in most cases to sufficiently precize results to work with for industrial use.

3.4. Growth Rate Dispersion. This phenomenon is the exhibition of different growth rates by crystals in a magma, even though they may have the same size and are exposed to identical conditions. It is now generally accepted that many observations originally attributed to size-dependent growth were due to growth rate dispersion. Such erroneous interpretations were the result of similarities in the effects of the two types of behavior on CSD (50,51).

The effects of growth rate dispersion on a population of sucrose crystals were first characterized by a linear correlation of the variance of the population about a mean size L with the extent of growth (48) . It was demonstrated later (52,53) that growth rate dispersion could account for anomalous characteristics in the population density of crystals obtained from continuous, steady-state crystallizers. Later studies examined batch crystallization data to show that apparent size-dependent growth of potassium alum crystals was a manifestation of growth rate dispersion (54). Crystals of citric acid monohydrate generated by contact nucleation were found to exhibit growth rate dispersion but not size-dependent growth (55,56).

Two distinctly different mechanisms leading to growth rate dispersion have experimental support. The first assumes that all crystals have the same time-averaged growth rate, but the growth rates of individual crystals fluctuate

about some mean value (57). Direct evidence of random fluctuations in growth rates has been reported for magnesium sulfate heptahydrate (58) and potassium alum (59). The second assumes that crystals are formed with a characteristic distribution of growth rates, but individual crystals retain a constant growth rate throughout their residence in a crystallizer. Findings on citric acid (55), potassium nitrate (60), and ammonium dihydrogen phosphate (61) support this mechanism.

Surface integration is thought to be the primary factor in both mechanisms of growth rate dispersion. The BCF theory indicates that the growth rate of a crystal face depends on the number, sign, and location of screw dislocations on the surface of a growing crystal. Collisions of crystals with each other and crystallizer internals result in changes in the dislocation network of a crystal, thereby leading to random fluctuations of growth rates. Changes in the dislocation networks also occur simply due to the imperfect growth of crystal faces. A distribution of growth rates is a result of the varying dislocation networks and densities among nuclei and seed crystals (56,62).

Although evidence exists for both mechanisms of growth rate dispersion, separate mathematical models were developed for incorporating the two mechanisms into descriptions of crystal populations: random growth rate fluctuations (57) and growth rate distributions (53,61). Both mechanisms can be included in a population balance to show the relative effects of the two mechanisms on crystal size distributions from batch and continuous crystallizers (63).

4. Crystal Characteristics

The morphology (including crystal shape or habit), size distribution, agglomeration, and purity of crystalline materials can determine the success in fulfilling the function of a crystallization operation.

4.1. Morphology. A crystal is highly organized and constituent units, which can be atoms, molecules, or ions, is positioned in a three-dimensional (3D) periodic pattern called a space group. A characteristic crystal shape results from the regular internal structure of the solid with crystal surfaces forming parallel to planes formed by the constituent units. The surfaces (faces) of a crystal may exhibit varying degrees of development, with a concomitant variation in macroscopic appearance.

If atoms, molecules, or ions of a unit cell are treated as points, the lattice structure of the entire crystal can be shown to be a multiplication in three dimensions of the unit cell. Only 14 possible lattices (called Bravais lattices) can be drawn in three dimensions. These can be classified into seven groups based on their elements of symmetry. Moreover, examination of the elements of symmetry (about a point, a line, or a plane) for a crystal shows that there are 32 different combinations (classes) that can be grouped into seven systems. The correspondence of these seven systems to the seven lattice groups is shown in Table 1.

The general shape of a crystal is referred to as its habit. The appearance of the crystalline product and its processing characteristics (such as washing and filtration) are affected by crystal habit. Relative growth rates of the faces of a crystal determine its shape. Faster growing faces become smaller than slower

Table 1. **The 14 Bravais Lattices**[a]

Type of symmetry	Lattice	Crystal system
cubic	cube	regular
	body-centered cube	
	face-centered cube	
tetragonal	square prism	tetragonal
	body-centered square prism	
orthorhombic	rectangular prism	orthorhombic
	body-centered rectangular prism	
	rhombic prism	
	body-centered rhombic prism	
monoclinic	monoclinic parallelepiped	monoclinic
	clinorhombic	
triclinic	triclinic parallelepiped	triclinic
rhomboidal	rhombohedron	triclinic
hexagonal	hexagonal prism	hexagonal

[a] Ref. 7.

growing faces and, in the extreme case, may disappear from the crystal altogether. Growth rates depend on the presence of impurities, rates of cooling, temperature, solvent, mixing, and supersaturation. Furthermore, the importance of each of these factors may vary from one crystal face to another. For example, consider Figure 11, which shows that the ⟨111⟩ face grows between 1.6 and 2.2 times as fast as the ⟨110⟩ face at the conditions examined. These results account for the elongated crystal shape exhibited by magnesium sulfate heptahydrate crystals. In addition, the effects of supersaturation and temperature are different on the growth rates of the two faces studied. Such behavior leads to changes in habit as the temperature and/or supersaturation are changed in a crystallizer.

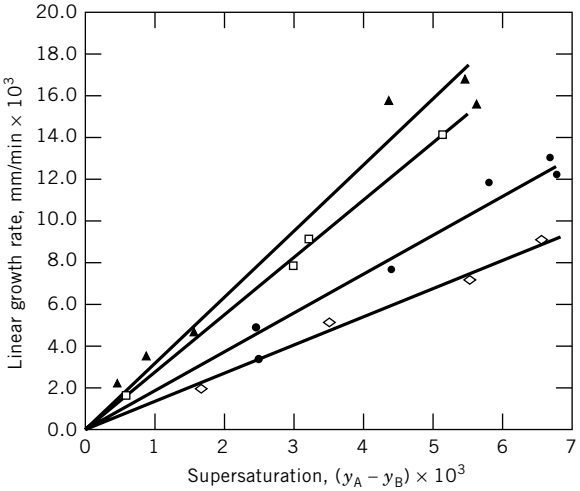

Fig. 11. Growth rate of faces of $MgSO_4 \cdot 7H_2O$. ▲, ⟨111⟩ face at $T_{sat} = 38.0°C$; ■, ⟨111⟩ face at $T_{sat} = 35.5°C$; ■, >110< face at $T_{sat} = 38.0°C$; ◆, >110< face at $T_{sat} = 33.5°C$; solution velocity = 1.2 cm/s (64). Reprinted with permission of the American Chemical Society.

A number of studies have shown that various additives can be included in a process stream to alter crystal habit (7). Prediction of such behavior is difficult and extensive laboratory or bench-scale experiments may be required to evaluate the effectiveness of habit modifiers (65). More recently, some measure of success has been achieved with altering the habit of organic crystals based on the molecular structure and forces between the crystallizing species or additive with a specific crystal face. Should an additive enhance the properties of a crystalline material, eg, by making it easier to filter, the expense associated with its use may be warranted. Significant efforts toward tailoring additives so that they have specific effects on crystal habit have been made by a number of research groups (66–73). The detailed understanding of the chemical interactions at the crystalline interface is necessary to determine the effect of additives on the crystal growth process. Chemical interactions include van der Waals, ionic, and hydrogen bonding. The influence of "tailor-made additives" on the habit of organic crystals was introduced by Lahav and co-workers (74) and coworkers from the Weizmann Institute, Israel in the 1980s. The reported effect for this group of additives is based on their structural similarity to the crystallizing units. The tailor-made additives are bound at preselected crystal faces and the structurally different sites that are exposed on distinct crystallographic faces. Thus the deposition of incoming crystal layers is hampered. The result is a growth rate reduction of the affected faces and a relative enlargement of its surface areas, since the slowest growing faces always dominate the crystal habit (75). The development of current computer software for molecular modeling or molecular simulations of crystal structures is based on Donnay and Harker (76) and Hartman and Perdok (77) and Hartman and Bennema (78) approaches. Meanwhile, a number of successful operations (see eg, (79–81)) is reported based on such computer works. Further developments are needed to save laboratory time and make faster progress in this still difficult and not finally established and understood field of crystallization.

Polymorphism is a condition in which chemically identical substances may crystallize into different forms (82). Each form is, however, only stable (thermodynamically) in a certain range of temperature and pressure. In the case of ambient pressure, eg, ammonium nitrate exhibits four changes in form (7) between-18- and 125°C:

$$\text{liquid} \xleftrightarrow{169{,}6^\circ\text{C}} \text{cubic} \xleftrightarrow{125{,}2^\circ\text{C}} \text{trigonal} \xleftrightarrow{84{,}2^\circ\text{C}} \text{orthorhombic I} \xleftrightarrow{32{,}3^\circ\text{C}} \text{orthorhombic II} \xleftrightarrow{-18^\circ\text{C}} \text{tetragonal} \qquad (30)$$

Transitions from one polymorphic form to another may be accompanied by changes in process conditions (temperature, pessure, shear or solution composition), transitions from one polymorphic form to another and lead to formation of a solid product with unacceptable properties (eg, melting point or dissolution rate).

A specific polymorph may be absolutely essential for a crystalline product, eg., one polymorph may have a more desirable color or greater hardness or disperse in water more easily than another polymorph. An interesting approach to keeping a thermodynamically nonstable polymorph from transforming to the

stable, but less desirable, polymorphic form uses an additive to block rearrangement of the molecular structure leading to the undesired form (83).

Pseudopolymorphs are solvates or in the case of water as solvent, hydrates, which means crystals that incooperate solvent molecules into the crystal lattic. Pseudopolymorphs exhibit different crystal forms and/or different densities, solubilities, dissolution rates, colors, hardnesses, etc. Compared with polymorphs, there is an additional degree of freedom (than temperature and pressure), which means a different solvent or even the moisture of the air that might change the stabile region of the pseudopolymorphe.

4.2. Agglomeration. Many of the analyses of industrial crystallizers require that the particle recovered from the crystallizer consist of a single crystal. Many of the properties of the crystal are affected deleteriously by agglomeration. Purity, eg, typically is diminished when agglomeration occurs. Countering the negative aspects of agglomeration is recognition that in many systems the single crystals produced by normal crystal growth would be too small to be separable using conventional solid–liquid separation equipment. In such instances, there would be no recoverable product without agglomeration.

A greater understanding of agglomeration is needed in at least two separate areas: identifying the variables affecting agglomeration and accounting for agglomeration properly in a population balance around a crystallizer. The latter of these has been addressed (84,85), but the subject matter is considered beyond the scope of the present discussion.

Several process variables that influence agglomeration of copper sulfate pentahydrate crystals have been identified (86). Particles originally appearing to be single crystals were found to be agglomerates of complex structure. Electron photomicrographs showed that the agglomerates were formed early in the life of crystals comprising the agglomerates and that the growth of these agglomerates had followed a complex and unpredictable pattern. The percentages of agglomerates recovered from a series of mixed-suspension, mixed-product experiments were found to increase with increasing supersaturation, increasing magma density, and decreasing agitation. The observations fit with a hypothesis that the agglomeration resulted when two or more crystals came together and were bonded through overgrowth of contact areas. Such a hypothesis is inadequate, however, in predicting when agglomeration will occur and the key variables that can be adjusted to control the agglomeration.

4.3. Purity. Although crystallization has been employed extensively as a separation process, purification techniques using crystallization have become of growing importance. Mechanisms by which impurities can be incorporated into crystalline products include adsorption of impurities on crystal surfaces (87), solvent entrapment in cracks, crevices and agglomerates, and inclusion of pockets of liquid (88,89). An impurity having a structure sufficiently similar to the material being crystallized can also be incorporated into the crystal lattice by substitution or entrapment (90,91) . Among these mechanisms, inclusion formation has been extensively studied (92–100). It has also been suggested that the purity may be directly linked to size and habit of product crystals, but the interaction does not appear to be simple. Note that the key to producing high purity crystals was to maintain the supersaturation at a low level so that large crystals were obtained (101). Others have found that reducing the size of

ammonium perchlorate crystals resulted in a substantial decrease in moisture due to inclusion (96).

A key factor in solving problems associated with crystal purity is identification of the mechanism of impurity in cooperation. Impurities are on the exterior of host crystals as a result of adsorption; wetting by a solvent that contains the impurities; or entrapment of impure solvent in cracks, crevices, agglomerates, and aggregates. Incorporation of impurities within crystals comes about through formation of inclusions (also referred to as occlusions) of solvent, lattice substitution, or lattice entrapment. Obviously, the characteristics of an impurity determine whether it is positioned on the surface or the interior of host crystals. Three key impurity types are solutes similar to the product, solutes dissimilar from the product, and the solvent. The effects of process variables on the purity of L-isoleucine crystallized from aqueous solutions containing other amino acids (impurities) have been determined (102). Another study has examined how the methanol content of L-serine crystals could be minimized when the mode of crystallization is addition of methanol to saturated aqueous solutions (4). Mixing and the rate at which supersaturation is generated are important in both of these cases.

4.4. Crystal Size Distributions. Particulate matter produced by crystallization has a size distribution that varies in a definite way over a specific size range. A CSD is most commonly expressed as a population (number) distribution relating the number of crystals at each size to a size or as a mass (weight) distribution expressing how mass is distributed over the size range. The two distributions are related and affect many aspects of crystal processing and properties, including appearance, solid–separation, purity, reactions, dissolution, and other properties involving surface area.

Population density (n) has the dimensions the number/(volume) (length). It is a key quantity in the discussion of CSD, a function of the characteristic crystal dimension L, and is defined so that it is independent of the magnitude of the system. When a total population density is used, the symbol is $\bar{n}$ and the units are number/length. Population density is defined by letting ΔN be the number of crystals per unit system volume in a size range from L to $L + \Delta L$, so that

$$n = \lim_{\Delta L \longrightarrow 0} \frac{\Delta N}{\Delta L} \tag{30}$$

The arbitrary system volume on which n is based must be defined before the population density function has meaning. For example, the volume may be that of the slurry or the clear liquor in the system.

The function N in equation 30 is a cumulative number distribution representing the number of crystals per unit volume in the distribution that have a characteristic dimension $<L'$. Therefore,

$$N(L') = \int_0^{L'} n dL \tag{31}$$

and the fraction of the crystals in the distribution $F(L')$ that have a size $<L'$ can be calculated as

$$F(L') = \frac{N(L')}{N_{\text{tot}}} \tag{32}$$

A mass (weight) density function, given the symbol m and having dimensions mass/(volume) (length), can be defined in manner analogous to population density; letting ΔM be the mass of crystals per unit system volume in the size range L to $L + \Delta$L,

$$m = \lim_{\Delta L \longrightarrow 0} \left\{ \frac{\Delta M}{\Delta L} \right\} \tag{33}$$

The two density functions can be related through a simple shape factor as follows. Suppose the mass of a single crystal is M_c and the characteristic dimension of that crystal is L. If the crystal is from a population in which shape is not a function of size, then the mass of any crystal from that population is related to characteristic dimension by a volume shape factor:

$$M_c = k_v \rho L^3 \tag{34}$$

Recognizing that the mass of crystals in a sample is the product of the number of crystals and the mass of a single crystal, mass and population densities may be related by the expression

$$\Delta M = k_v \rho L^3 \Delta N \tag{35}$$

where ρ is crystal density. Dividing by ΔL and taking the limit as this quantity approaches zero,

$$m = k_v \rho L^3 n \tag{36}$$

The function M used in the above equations is a cumulative mass distribution function, representing the mass of crystals having a characteristic dimension $<L'$. The total mass of crystals per unit volume is related to population density by the equation

$$M_T = k_v \rho \int_0^\infty L^3 n dL \tag{37}$$

This quantity, which is often referred to as magma density or solids concentration (mass of crystals per unit system volume), is often an important process variable. A cumulative mass fraction of crystals having a size $<L'$ can also be defined as

$$W(L') = \frac{M(L')}{M_T} = \frac{k_v \rho \int_0^{L'} L^3 n(L) dL}{M_T} \tag{38}$$

Moments of a distribution often provide information that can be used to characterize particulate matter. The jth moment of the population density function n is defined as

$$m_j = j\text{th moment} = \int_0^\infty L^j n \, dL \tag{39}$$

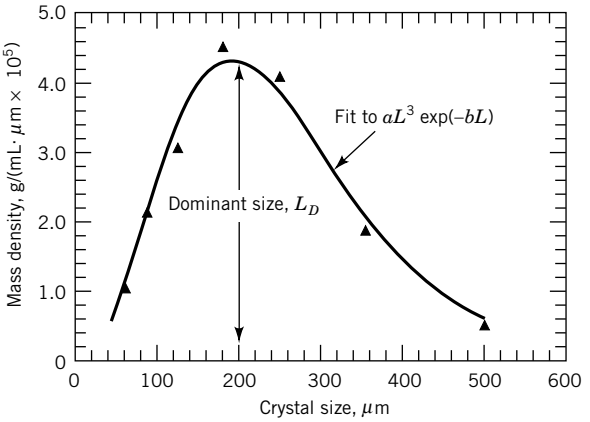

Fig. 12. Determination L_D from plot of mass density function.

It can be demonstrated that the total number of crystals, the total length, the total area, and the total volume of crystals, all in a unit of system volume, can be evaluated from the zero, first, second, and third moments of the population density function.

An average crystal size can be used to characterize a CSD. However, the average can be determined on any of several bases, and the basis selected must be specified for the average to be useful. More than 20 different averaging procedures have been proposed, yet none is generally satisfactory or preferred (7).

The complete characterization of a particulate material requires development of a functional relationship between crystal size and population or mass. The functional relationship may assume an analytical form (9), but more frequently it is necessary to work with data that do not fit such expressions. As such detail may be cumbersome or unavailable for a crystalline product, the material may be more simply (and less completely) described in terms of a single-crystal size and a spread of the distribution about that specified dimension.

The dominant crystal size, L_D, is most often used as a representation of the product size, because it represents the size about which most of the mass in the distribution is clustered. If the mass density function defined in equation 33 is plotted for a set of hypothetical data as shown in Figure 12, it would typically be observed to have a maximum at the dominant crystal size. In other words, the dominant crystal size L_D is that characteristic crystal dimension at which $dm/dL = 0$. Also shown in Figure 12 is the theoretical result obtained when the mass density is determined for a perfectly mixed, continuous crystallizer within which invariant crystal growth occurs. That is, mass density is found for such systems to follow a relationship of the form $m = a\ L^3\exp(-bL)$, where a and b are system-dependent parameters.

The coefficient of variation (cv) of a distribution is a measure of the spread of the distribution about some characteristic size. It is often used in conjunction with dominant size to characterize crystal populations through the equation

$$cv = \frac{\sigma}{L_D} \tag{40}$$

where σ is the standard deviation of the distribution. The coefficient of variation of the mass density function about the dominant crystal size is given by

$$cv = \left(\frac{m_3 m_5}{m_4^2} - 1\right)^{1/2} \tag{41}$$

where m_i are defined in equation 39.

5. Population Balances and Crystal Size Distributions

Population balances and crystallization kinetics may be used to relate process variables to the CSD produced by the crystallizer. Such balances are coupled to the more familiar balances on mass and energy. It is assumed that the population distribution is a continuous function and that crystal size, surface area, and volume can be described by a characteristic dimension L. Area and volume shape factors are assumed to be constant, which is to say that the morphology of the crystal does not change with size.

A balance is formulated around a control volume V_T on the number of crystals in any size range, say L_1 to L_2. It must account for crystals that enter and leave the size range by convective flow and crystals that enter and leave the size range by crystal growth. Crystal breakage and agglomeration are assumed to be negligible in the present analysis, and it is assumed that crystals are formed by nucleation at size zero. The rate of crystal growth G is defined as the rate of change of the characteristic crystal dimension L; ie, $G = dL/dt$.

Consider the crystallizer shown in Figure 13. If it is assumed that the crystallizer is well mixed with a constant slurry volume V_T, then, as shown (9), the following partial differential population balance can be derived

$$\frac{\partial(nG)}{\partial L} + \frac{Q_0 n}{V_T} - \frac{Q_i n_i}{V_T} = -\frac{\partial n}{\partial t} \tag{42}$$

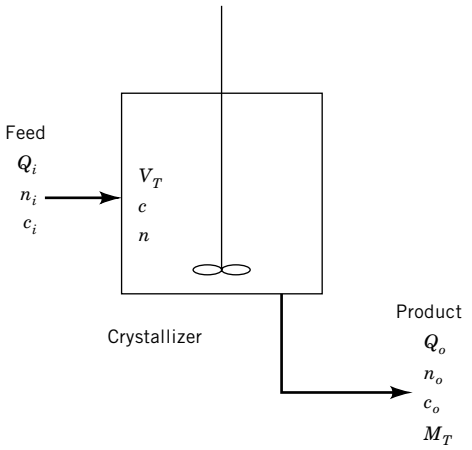

Fig. 13. Schematic diagram of a simple, perfectly mixed crystallizer.

If the crystallizer is now assumed to operate with a clear feed ($n_i = 0$), at steady state ($\partial n/\partial t = 0$), and if the crystal growth rate G is invariant and a mean residence time τ is defined as V_T/Q_0, then the population balance can be written as

$$G\frac{dn}{dL} + \frac{n}{\tau} = 0 \tag{43}$$

τ is often referred to as the drawdown time (retention time) to reflect that it is the time required to empty the contents from the crystallizer if the feed is set to zero. Equation 43 can be integrated using the boundary condition $n = n^0$ at $L = 0$:

$$n = n^0 \exp\left(-\frac{L}{G\tau}\right) \tag{44}$$

If the magma volume V_T is allowed to vary in the system on which equation 42 is based, the population balance becomes

$$\frac{\partial n}{\partial t} + \frac{\partial (nG)}{\partial L} + n\,\frac{\partial (\ln V_T)}{\partial t} + \frac{Q_0 n}{V_T} = 0 \tag{45}$$

The crystallizer model that led to the development of equations 44 and 45 is referred to as the mixed-suspension, mixed-product removal (MSMPR) crystallizer.

5.1. Determination of Crystallization Kinetics. Under steady-state conditions, the total number production rate of crystals in a perfectly mixed crystallizer is identical to the nucleation rate, B^0. Accordingly,

$$B^0 = \frac{1}{\tau}\int_0^\infty n\,dL \tag{46}$$

For crystallizers following the constraints leading to equation 44,

$$B^0 = n^0 G \tag{47}$$

Combining equations 44 and 47

$$n = \frac{B^0}{G}\exp\left(-\frac{L}{G\tau}\right) \tag{48}$$

Analysis of equation 48 shows that a single sample taken either from inside the crystallizer or from the product stream will allow evaluation of nucleation and growth rates at the system conditions. Figure 14 shows a plot of typical population density data obtained from a crystallizer meeting the stated assumptions. The slope of the plot of such data may be used to obtain the growth rate, and the product of the intercept and growth rate gives the nucleation rate.

Many industrial crystallizers operate in a well-mixed or nearly well-mixed manner, and the equations derived above can be used to describe their performance. Furthermore, the simplicity of the equations describing an MSMPR

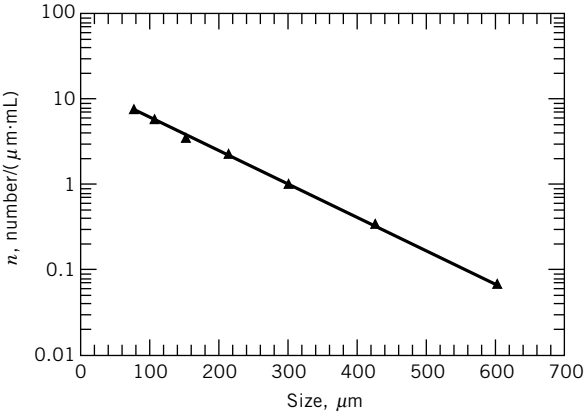

Fig. 14. Plot of population density as a function of size for KNO_3 $\tau = 15$ min. For the line, $n = 16.528^*$ exp $(-0.0090426L)$; $R = 0.99752$; slope $= -1/G\tau$; intercept $= n^0 = B^0/G$.

crystallizer make experimental equipment configured to meet the assumptions leading to equation 44 useful in determining nucleation and growth kinetics in systems of interest.

From a series of runs at different operating conditions, a correlation of nucleation and growth kinetics with appropriate process variables can be obtained; the resulting correlation can then be used to guide either crystallizer scaleup or the development of an operating strategy for an existing crystallizer. The variables affecting nucleation and growth kinetics include temperature, supersaturation, magma density, and external stimuli, such as agitation or circulation rate of the magma. Empirical power-law functions are used most frequently in correlating nucleation and growth rates, but the choice of the independent variables can be justified from a mechanistic perspective. For example, systems that are believed to follow secondary nucleation mechanisms should include a variable such as magma density, which reflects the concentration of crystals in the crystallizer. The most commonly used power-law functions are

$$B^0 = k_1 s^b M_T^j \tag{49}$$

$$G = k_2 s^g \tag{50}$$

It is often difficult to measure supersaturation, especially in systems that have high growth rates. Even though the supersaturation in such systems is so small that it can be neglected in writing a solute mass balance, it is important in calculating nucleation and growth rates. In such instances, it is convenient to substitute growth rate for supersaturation by combining equations 49 and 50 to yield

$$B^0 = k_n G^n M_T^j \tag{51}$$

The constant k_n may depend on process variables such as temperature, rate of agitation or circulation, presence of impurities, and other variables. If

sufficient data are available, such quantities may be separated from the constant by adding more terms in a power-law correlation. The term k_n is specific to the operating equipment and generally is not transferrable from one equipment scale to another. The system-specific constants j and g are obtainable from experimental data and may be used in scaleup, although j may vary considerably with mixing conditions. Illustration of the use of data from a commercial crystallizer to obtain the kinetic parameters k_n, j, and j is available (103).

5.2. Mass Balance Constraints. The following mass balance on solute can be constructed from the schematic diagram of a continuous crystallizer shown in Figure 13:

$$Q_i c_i = Q_0 c_0 + Q_0 M_T \tag{52}$$

c_0 is determined by system kinetics and constrained by a solid–liquid equilibrium (solubility) relationship, which gives the equilibrium concentration c^* at the system conditions. The system (solute–solvent and crystallizer) is characterized by the magnitude of the supersaturation $(c_0 - c^*)$ remaining in the solution exiting the crystallizer. If the mass balance is closed by substituting c^* for c_0 in equation 52, the system is said to be a fast-growth or class II system. If the mass balance is not closed, significant supersaturation remains in the solution, the system is said to be a slow-growth or class I system. In other words, for class I (slow-growth) systems: $c_0 > c^*$ and

$$M_T = \frac{Q_i}{Q_0} c_i - c_0 \tag{53}$$

Values of process variables such as residence time will change the system kinetics that change c_0 and, in turn, M_T.

For class II (fast-growth) systems: $c_0 = c^*$ and

$$M_T = \frac{Q_i}{Q_0} = c_i - c^* \tag{54}$$

Process variables do not change c^* and, therefore, M_T is constant over modest ranges of operating conditions.

5.3. CSD Characteristics for MSMPR Crystallizers. The perfectly mixed crystallizer described in the preceding discussion is highly constrained and the functional form of CSD produced by such systems is fixed. Such distributions have the following characteristics:

1. Moments of the distribution can be calculated for MSMPR crystallizers by the simple expression

$$m_j = j \ln^0 (G\tau)^{j+1} \tag{55}$$

Properties of the distribution such as total number of crystals per unit volume, total length of crystals per unit volume, total area of crystals per unit volume, and total volume of solids (crystals) per unit volume may be explicitly evaluated from the moment equations.

2. The dominant crystal size L_D is given by $L_D = 3\ G\tau$. This quantity is also the ratio m_3/m_2, which is often given the symbol $\bar{L}\bar{L}_{3,2}$.
3. From the definition of the coefficient of variation given by equation 41, cv = 50% for an MSMPR crystallizer. Such a cv may be too large for certain commercial products, which means either the crystallizer must be altered or the product must be screened to separate the desired fraction.
4. The magma density M_T (mass of crystals per unit volume of slurry or liquor) may be obtained from the third moment of the population density function and is given by

$$M_T = 6\rho k_v n^0 (G\tau)^4 \tag{56}$$

Although magma density is a function of the kinetic parameters n^0 and G, it often can be measured independently. In such cases, it should be used as a constraint in evaluating nucleation and growth rates from measured CSDs (101), especially if the system of interest exhibits the characteristics of anomalous crystal growth.

5. Kinetic parameters for nucleation and growth rate can be used to predict the CSD for a given set of crystallizer operating conditions. Variation in one of the kinetic parameters without changing the other is not possible. Accordingly, the relationship between these parameters determines the ability to alter the characteristic properties (such as dominant size) of the distribution obtained from an MSMPR crystallizer (9).

5.4. Preferential Removal of Crystals. Crystal size distributions produced in a perfectly mixed continuous crystallizer are highly constrained; the form of the CSD in such systems is determined entirely by the residence time distribution of a perfectly mixed crystallizer. Greater flexibility can be obtained through introduction of selective removal devices that alter the residence time distribution of materials flowing from the crystallizer. The role of classified removal is best described in terms of idealized models of clear-liquor advance, classified-fines removal, and classified-product removal.

Clear-liquor advance is simply the removal of mother liquor from the crystallizer without simultaneous removal of crystals. The primary objective of *fines removal* is preferential withdrawal from the crystallizer of crystals whose size is below some specified value. Such crystals may be redissolved and the resulting solution returned to the crystallizer. *Classified-product removal* is carried out to remove preferentially those crystals whose size is larger than some specified value.

The effects of each selective removal function on CSD can be described in terms of the population density function n. It is convenient to define flow rates in terms of clear liquor, which requires the population's density function to be defined on a clear-liquor basis. In the present discussion, only systems exhibiting invariant crystal growth are considered.

Clear-liquor advance reduces the quantity of liquor that must be processed by solid–liquid separation equipment (eg, a filter or a centrifuge). The reduction in liquor flow through the separation equipment may allow use of smaller equipment for a fixed production rate or increased production through fixed equipment.

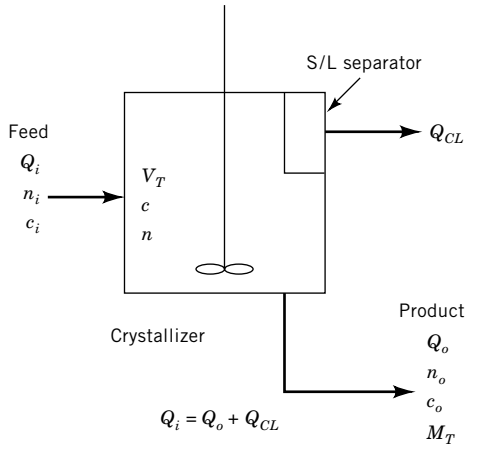

Fig. 15. Simplified schematic diagram of clear-liquor advance or double-draw off (DDO).

The function of clear-liquor advance can be illustrated by considering a simple operation, shown in Figure 15, in which Q_i, Q_{CL}, and Q_0 represent volumetric flow rates of clear-liquor fed to the crystallizer, in the clear-liquor advance, and in the output slurry. In such systems the population density function is given by the expression

$$n = n^0 \exp\left(-\frac{L}{G\tau_p}\right) \tag{57}$$

where $\tau_p = V/Q_0$. It is clear that increasing Q_{CL} decreases Q_0 and thereby increases the residence time of the crystals in the crystallizer.

Clearly, the form of the population density function resulting from a clear-liquor advance system is identical to that expected from perfectly mixed systems in which $\tau_{crystals}$ are identical to τ_{liquor}. Unless the increase in magma density associated with clear-liquor advance results in significant increases in nucleation, some increase in the dominant crystal size can be expected. It has been observed that the increase in L_D may be greater than predicted from theory. This is caused by the stream being removed as clear liquor containing varying amounts of fines, which means the system characteristics are those of classified-fines removal.

As an idealization of the classified-fines removal operation, assume that two streams are withdrawn from the crystallizer, one corresponding to the product stream and the other to a fines removal stream. Such an arrangement is shown schematically in Figure 16. The flow rate of the clear solution in the product stream is designated Q_0 and the flow rate of the clear solution in the fines removal stream is set as $(R-1)\ Q_0$. Furthermore, assume that the device used to separate fines from larger crystals functions so that only crystals below an arbitrary size L_F are in the fines removal stream and that all crystals below size L_F have an equal probability of being removed in the fines removal stream. Under these conditions, the CSD is characterized by two mean residence

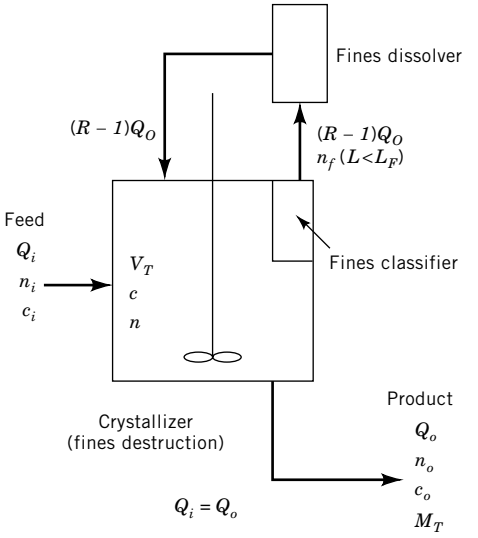

Fig. 16. Simplified schematic diagram of classified-fines removal.

times, one for the fines and the other for crystals larger than L_F. These quantities are related by the equations

$$\tau_F = \frac{V}{RQ_0} = \frac{\tau}{R} \quad \text{for} \quad L < L_F \tag{58}$$

$$\tau = \frac{V}{Q_0} \quad \text{for} \quad L \geq L_F \tag{59}$$

where V is the volume of clear solution in the crystallizer. The ratio of the probability of a crystal $<L_F$ being removed from the crystallizer to that of crystals $>L_F$ being removed is $R = \tau/\tau_F$.

For systems following invariant growth, the crystal population density in each size range decays exponentially with the inverse of the product of growth rate and residence time. For a continuous distribution, the population densities of the classified fines and the product crystals must be the same at size L_F. Accordingly, the population density for a crystallizer operating with classified-fines removal is given by

$$n = n^\circ \exp\left[-\frac{RL}{G\tau}\right] \quad \text{for} \quad L \leq L_F \tag{60}$$

$$n = n^\circ \exp\left[-\frac{(R-1)L_F}{G\tau}\right] \exp\left[-\frac{L}{G\tau}\right] \quad \text{for} \quad L > L_F \tag{61}$$

Figure 17 shows how the population density function changes with the addition of classified-fines removal. It is apparent from the figure that fines removal

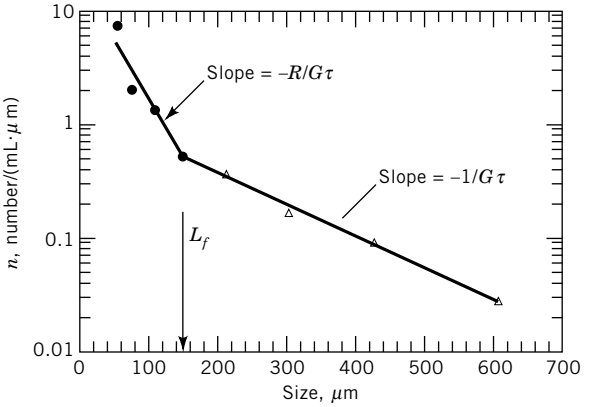

Fig. 17. Population density function for product from crystallizer with classified-fines removal. Cut size $L_F = 150$ μm; $R = 3.7$.

increases the dominant crystal size, but it also increases the spread of the distribution.

A simple method for implementation of classified-fines removal is to remove slurry from a settling zone in the crystallizer. The settling zone can be created by constructing a baffle that separates the zone from the well-mixed portion of the vessel, as is the case for a draft-tube-baffle crystallizer, or in small-scale systems, by simply inserting a length of pipe into the crystallizer chamber. The separation of crystals in the settling zone is based on the dependence of settling velocity on crystal size; only those crystals having a settling velocity greater than the upward velocity of the slurry remain in the crystallizer. As the cross-sectional area of a settling zone is invariant, the flow rate of slurry through the zone determines the cut size L_F, and it also determines the parameter R used in equations 58–61.

Classified removal of course material also can be used, as shown in Figure 18. In a crystallizer equipped with idealized classified-product removal, crystals above some size L_C are removed at a rate Z times the removal rate expected for a perfectly mixed crystallizer, and crystals $>L_C$ are not removed at all. Larger crystals can be removed selectively through the use of an elutriation leg, hydrocyclones, or screens. By using the analysis of classified-fines removal systems as a guide, it can be shown that the crystal population density within the crystallizer magma is given by the equations

$$n = n^0 \exp\left[-\frac{L}{G\tau}\right] \quad \text{for} \quad L \leq L_C \tag{62}$$

$$n = n^0 \exp\left[\frac{(Z-1)L_C}{G\tau}\right] \exp\left[-\frac{ZL}{G\tau}\right] \quad \text{for} \quad L > L_C \tag{63}$$

where τ is defined as the residence time V/Q_0. Figure 19 shows the effects of classified-product removal on crystal size distribution. The characteristics of the

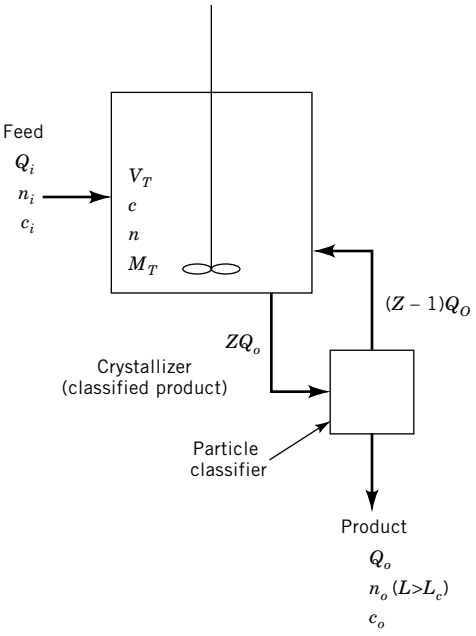

Fig. 18. Classified withdrawal of course crystals.

CSD obtained from a system with classified product removal show a narrower distribution (reduced coefficient of variation) and smaller dominant size. A more complete discussion of the implications of classified-product removal, with particular attention given to the distinction between the crystal population densities within the crystallizer and in the product has been given (9).

It is possible to obtain both a narrowing of the distribution and an increase in dominant size by combining preferential removal of fines and course crystals.

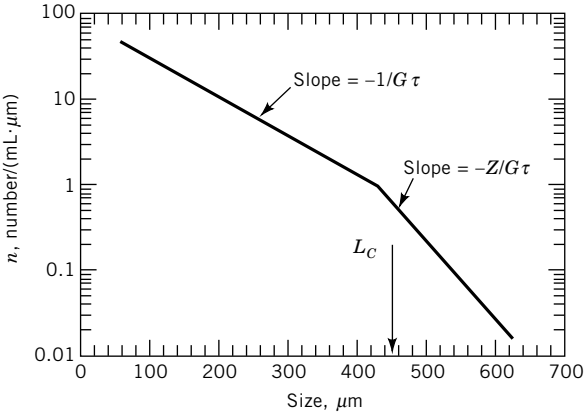

Fig. 19. Effect of classified-product removal on population densities within a crystallizer and in the crystallizer product.

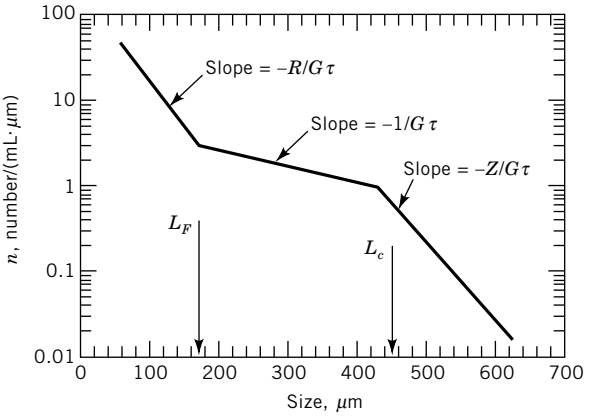

Fig. 20. Population density functions of crystals within a crystallizer, having both classified-fines and classified-product removal and of crystals in the product from such a crystallizer.

Including the idealized removal functions for fines and course crystals in a population balance and assuming invariant crystal growth will result in a population density function within the crystallizer given by equations 64–66, Figure 20 illustrates the effects of both removal functions on population density. This plot of population density results from sampling the magma within a crystallizer, not from sampling the product stream.

$$n = n^0 \exp\left[-\frac{RL}{G\tau}\right] \quad \text{for} \quad L \leq L_F \tag{64}$$

$$n = n^0 \exp\left[-\frac{(R-1)L_F}{G\tau}\right] \exp\left[-\frac{L}{G\tau}\right] \quad \text{for} \quad L_F < L < L_C \tag{65}$$

$$n = n^0 \exp\left[-\frac{(R-1)L_F}{G\tau}\right] \exp\left[\frac{(Z-1)L_C}{G\tau}\right] \exp\left[-\frac{ZL}{G\tau}\right] \quad \text{for} \quad L \geq L_C \tag{66}$$

The model of the crystallizer and selective removal devices that led to equations 64–66 is referred to as the R–Z crystallizer. It is an obvious idealization of actual crystallizers because of the perfect cuts assumed at L_F and L_C. However, it is a useful approximation to many systems and it allows qualitative analyses of complex operations. The R–Z model may also be representative of inadvertent classification, ie, fines or course crystals may be preferentially removed from a crystallizer without installation of specific hardware to accomplish such an objective.

Although many commercial crystallizers operate with some form of selective crystal removal, such devices can be difficult to operate because of fouling of heat exchanger surfaces or blinding of screens. In addition, several investigations identify interactions between classified fines and course product removal as

causes of cycling of a CSD (9). Often such behavior can be minimized or even eliminated by increasing the fines removal rate (104–106).

5.5. Batch Crystallization. Crystal size distributions obtained from batch crystallizers are affected by the mode used to generate supersaturation and the rate at which supersaturation is generated. For example, in a cooling mode there are several routes that can be followed in reducing the temperature of the batch system, and the same can be said for the generation of supersaturation by evaporation or by addition of an antisolvent or precipitant. The complexity of a batch operation can be illustrated by considering the summaries of seeded and unseeded operations shown in Figure 21.

The CSDs resulting from the operating strategies outlined in Figure 21 depend greatly on the use of seeding, the rate at which supersaturation is generated, and those variables that are important in the prevailing mechanism of nucleation. Figures 22 and 23 summarize the qualitative variations in CSD that may be observed in batch crystallization and the role of adding seed crystals to such systems (107–109).

More quantitative relationships of the CSD obtained from batch operations can be developed through formulation of a population balance. By using a population density defined in terms of the total crystallizer volume rather than on a specific basis ($\bar{n} = nV$), the general population balance given by equation 42 can be modified in recognition of there being no feed or product streams:

$$\frac{\partial(nV)}{\partial T} + \frac{\partial(GnV)}{\partial L} = \frac{\partial \bar{n}}{\partial t} + \frac{\partial(G\bar{n})}{\partial L} = 0 \tag{67}$$

The solution to equation 67 requires an initial condition ($\bar{n}$ at $t = 0$) and a boundary condition ($\bar{n}$ at a specific value of L). Assuming that crystals are formed at

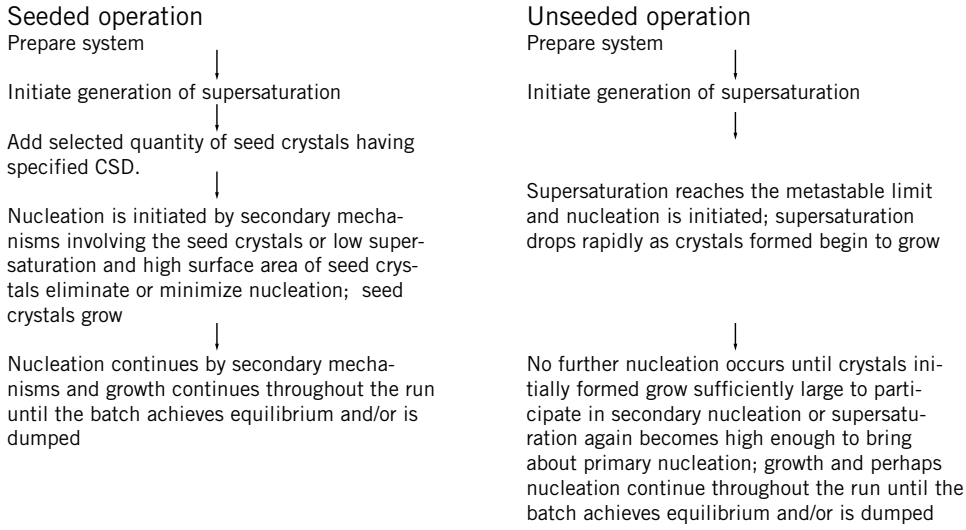

Fig. 21. Batch crystallizer operation.

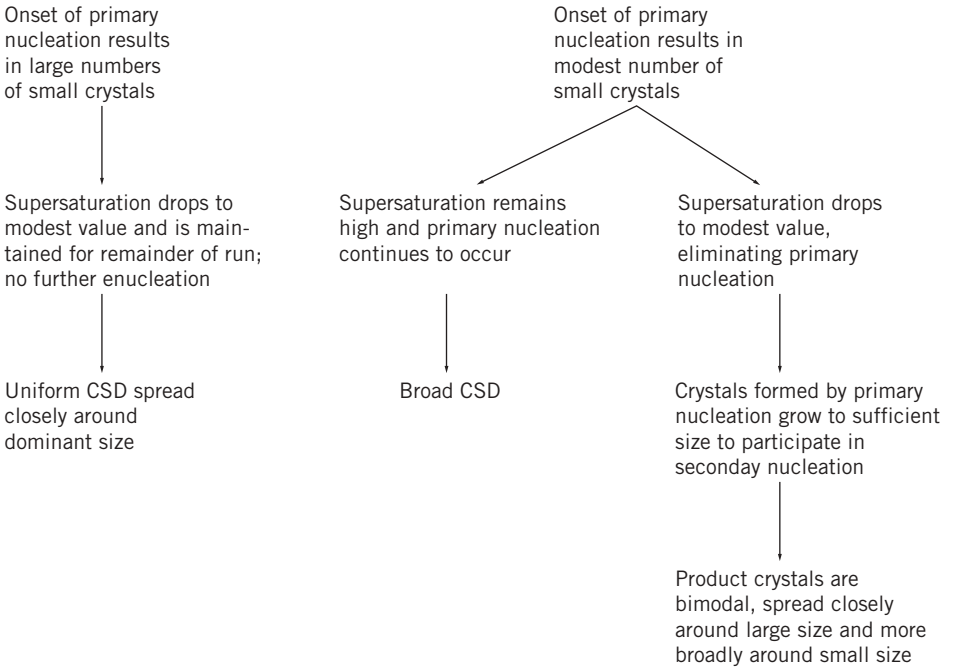

Fig. 22. CSD characteristics from batch crystallization without seeding.

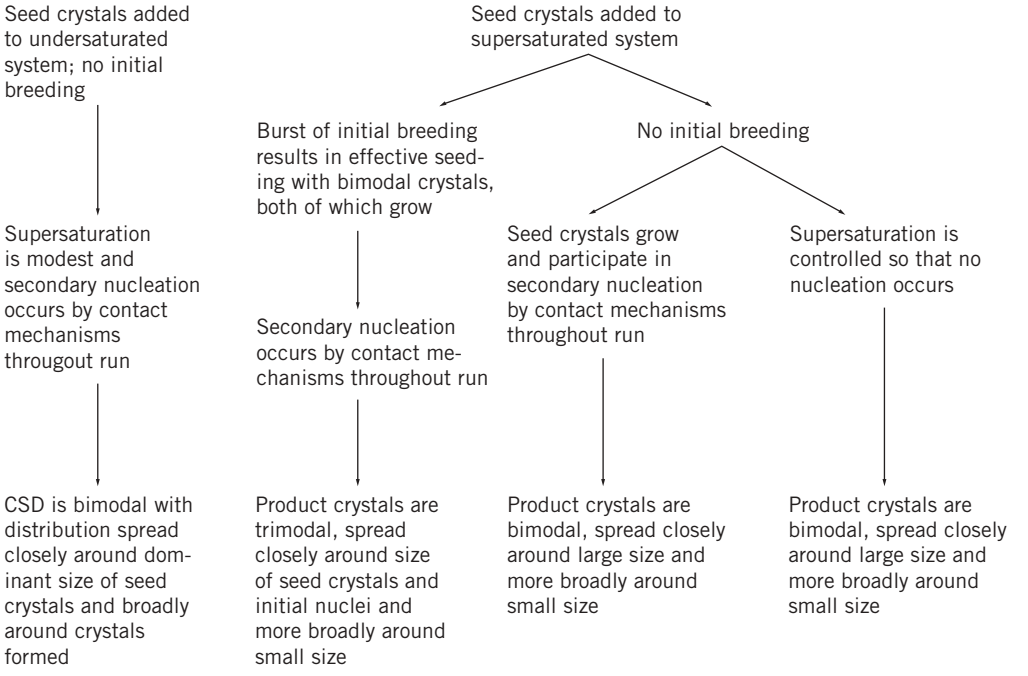

Fig. 23. CSD characteristics from batch crystallization with seeding.

zero size gives the boundary condition:

$$\bar{n}(0,t) = \bar{n}^0(t) = \frac{\bar{B}^0(t)}{G(0,t)} \tag{68}$$

Identification of an initial condition is difficult because of the problem of specifying the size distribution at the instant nucleation occurs. The difficulty is mitigated through the use of seeding, which would mean that the initial population density function would correspond to that of the seed crystals:

$$\bar{n}(\mathrm{L},0) = \bar{n}_S(L) \tag{69}$$

where $\bar{n}_s$ is the population density function of the seed crystals.

Moments of the population density function, which are given by

$$\bar{m}_j = \int_0^\infty L^j \bar{n} dL \tag{70}$$

are especially useful in modeling CSDs in batch operations and in the development of equations relating a control variable to time. By recognizing that the zero moment is the total number of crystals in the system, it can be shown that

$$\frac{d\bar{m}_0}{dt} = \bar{n}^0 G = \bar{B}^0 = \frac{d\bar{N}_T}{dt} \tag{71}$$

The following equations can be derived from the relationships of moments to properties of the distribution:

$$\frac{d\bar{m}_1}{dt} = G\bar{m}_0 \Longrightarrow \frac{d\bar{L}_T}{dt} = \bar{N}_T G \tag{72}$$

$$\frac{d\bar{m}_2}{dt} = 2G\bar{m}_1 \Longrightarrow \frac{d\bar{A}_T}{dt} = 2k_a \bar{L}_T G \tag{73}$$

$$\frac{d\bar{m}_3}{dt} = 3G\bar{m}_2 \Longrightarrow \frac{d\bar{M}_T}{dt} = 3\left(\frac{k_v}{k_a}\right)\rho \bar{A}_T G \tag{74}$$

where $\bar{N}\bar{N}_T$ is total number of crystals, $\bar{L}\bar{L}_T$ is total crystal length, $\bar{A}_T$ is total surface area of the crystals, and $\bar{M}\bar{M}_T$ is total mass of crystals in the crystallizer. A solute balance must also be satisfied.

$$\frac{d(V_C)}{dt} + \frac{d\bar{M}_T}{dt} = 0 \tag{75}$$

where V is the system volume, and c is solute concentration in the solution.

Control of supersaturation is an important factor in obtaining the CSDs of desired characteristics, and it would be useful to have a model relating the rate of

cooling or evaporation or addition of diluent required to maintain a specified supersaturation in the crystallizer. Contrast this to the uncontrolled situation of natural cooling in which the heat transfer rate is given by

$$Q = UA(T - T_c) \tag{76}$$

where U is a heat-transfer coefficient, A is the area available for heat transfer, T is the temperature of the magma, and T_c is the temperature of the cooling fluid. If U and T_c are constants, the maximum heat-transfer rate and the highest rate at which supersaturation is generated are at the beginning of the process when T is highest. These conditions can lead to excessive primary nucleation and the formation of incrustations on the heat-transfer surfaces.

Better product characteristics are obtained through control of the rate at which supersaturation (cooling, evaporation, and addition of an antisolvent or precipitant) is generated (110). An objective of the operation may be to maintain the supersaturation at some constant prescribed value, usually below the metastable limit associated with primary nucleation. For example, the batch may be cooled slowly at the beginning of the cycle and more rapidly at the end. This can be seen in Figure 24 for natural cooling versus controlled cooling of a batch crystallizer. Natural cooling is shown (in **a**) resulting in changeable compared to constant supersaturation (see **b**) (111). With appropriate sensors, supersaturation

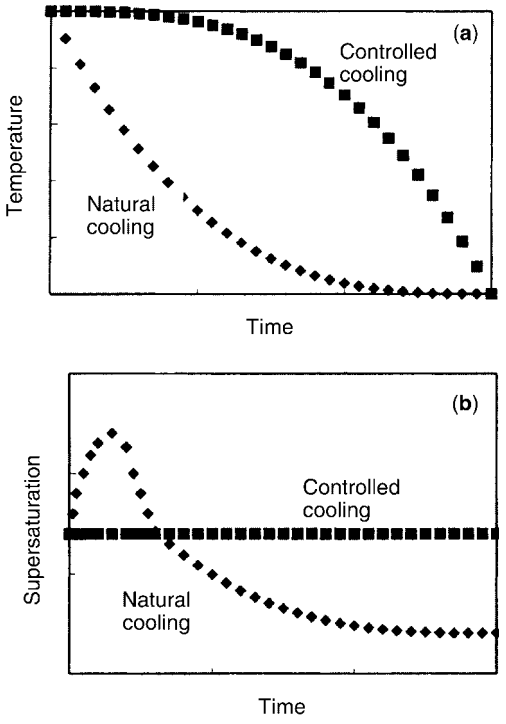

Fig. 24. Natural and controlled cooling batch crystallization: (**a**) Temperature profile, (**b**) Supersaturation profile (111).

can be measured in-line and thereby the actual supersaturation can be controlled. Ultrasound (112,113) as well as infrared (ir) spectroscopy (114) are sensor options.

Formulations of population balances on batch crystallizers have been illustrated, and a variety of operating strategies have been considered (115). The results are often complex and present difficult control schemes at best. For example, suppose a model is needed to guide the operation of a batch seeded crystallizer so that isothermal solvent evaporation can be accomplished at a rate that gives a constant crystal growth rate and no nucleation. It is shown that the evaporation rate required is a cubic function of time and the corresponding rate of heat input to the crystallizer must be controlled accordingly. If cooling was to be used rather than evaporation, a similar analysis would show that the dependence of crystallizer temperature on time is highly nonlinear. Although the development of a strategy for generating supersaturation can be aided by such analyses, the initial conditions in the models derived are based on properties of seed crystals added to the crystallizer.

The advantages of selective removal of fines from a batch crystallizer have been demonstrated (116,117). These experimental programs showed narrowing of CSDs and suggest significant reductions in the fraction of a product that would consist of fines or undersize material.

6. Crystallizers and Crystallization Operations

Crystallization equipment can vary in sophistication from a simple stirred tank to a complicated multiphase column, and the operation can range from allowing a vat of liquor to cool through exchanging heat with the surroundings to the complex control required of batch cyclic operations. In principle, the objectives of these systems are all the same: to produce a pure product at a high yield in an acceptable retention time with, in many cases, a desired CSD. However, the characteristics of the crystallizing system and desired properties of the product often dictate that a specific crystallizer be used in a particular operating mode.

6.1. Crystallization from Solution. Crystallization techniques are related to the methods used to induce a driving force for solids formation and to the medium from which crystals are obtained. Several approaches are defined in the following discussion.

Cooling crystallizers use a heat sink to remove both sensible heat from the feed stream and the heat of crystallization released as crystals are formed. The heat sink may be no more than the ambient surroundings of a batch crystallizer, or it may be cooling water or another process stream.

Evaporative crystallizers generate supersaturation by removing solvent, thereby increasing solute concentration. These crystallizers may be operated under vacuum, and, in such circumstances, it is necessary to have a vacuum pump or ejector as a part of the unit. If the boiling point elevation of the system is low (ie, the difference between the boiling point of a solution in the crystallizer and the condensation temperature of pure solvent at the system pressure), mechanical recompression of the vapor obtained from solvent evaporation can be used to produce a heat source to drive the operation.

Evaporative-cooling crystallizers are fed with a liquor that is at a temperature above that in the crystallizer. As the feed is introduced to the crystallizer, which is at a reduced pressure, solvent flashes, thereby concentrating the solute in the resulting solution and reducing the temperature of the magma. The mode of this operation can be degenerated to that of a simple cooling crystallizer by returning condensed solvent to the crystallizer body.

Salting-out or antisolvent crystallization operates through the addition of a salt, polymer, or antisolvent to the magma in a crystallizer. The selection of the nonsolvent is based on the effect of the solvent on solubility (it reduces the solubility in the solvent of the material to be crystalline), cost, properties that affect handling, interaction with product requirements, and ease of recovery. The effect of adding a nonsolvent can be quite complex, as it increases the volume required for a given residence time and may produce a highly nonideal mixture of solvent, nonsolvent, and solute from which the solvent is difficult to separate.

Reactive crystallization (118) addresses those operations in which a reaction occurs to produce a crystallizing solute. The concentration of the solute formed generally is greater than that corresponding to solubility. In a subset of systems, the solubility is nearly zero and, concomitantly, the supersaturation produced by reaction is large. These are often referred to as *precipitation* operations (119), and CSDs from them contain a large fraction of fine crystals.

Supercritical fluid solvents are those formed by operating a system above the critical conditions of the solvent. Solubilities of many solutes in such fluids often is much greater than those found for the same solutes but with the fluid at subatmospheric conditions. Recently, there has been considerable interest in using supercritical fluids as solvents in the production of certain crystalline materials because of the special properties of the product crystals. Rapid expansion of a supercritical system rapidly reduces the solubility of a solute throughout the entire mixture. The resulting high supersaturation produces fine crystals of relatively uniform size. Moreover, the solvent poses no purification problems because it simply becomes a gas as the system conditions are reduced below critical (120–123).

6.2. Crystallizers. The basic requirements of a system involving crystallization from solution are as follows: (*1*) a means of generating supersaturation in a fashion commensurate with the requirements of producing a satisfactory CSD, (*2*) a vessel to provide sufficient residence time for crystals to grow to a desired size, and (*3*) mixing to provide a uniform environment for crystal growth. There are numerous manufacturers of crystallization equipment; in addition, many chemical companies design their own crystallizers based on expertise developed within their organizations. Rather than attempt to describe the variety of special crystallizers that can be found in the marketplace, this section provides a brief general survey of types of crystallizers that use the modes outlined above. Greater detail can be found in the literature (124–127).

The forced-circulation crystallizer is a simple unit designed to provide high heat-transfer coefficients in either an evaporative or a cooling mode. Figure 25 shows a schematic diagram of a forced-circulation crystallizer that withdraws a slurry from the crystallizer body and pumps it through a heat exchanger where heat may be either added to or removed from the slurry. Heat transferred to the circulating magma causes evaporation of solvent as the magma is returned

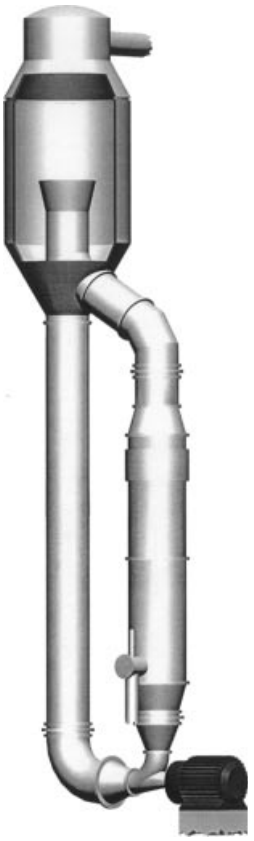

Fig. 25. Forced circulation crystallizers (Messo-FC, Messo Chemietechnik GmbH).

to the crystallizer, whereas heat removal lowers the temperature of the circulating magma. Forced circulation is used to control circulation rates and velocities past the heat-transfer surfaces conditions.

When cooling is the selected mode by which supersaturation is generated, heat can be transferred through an external cooling surface, as shown in Figure 25, or through coils or a jacket internal to the crystallizer body. The higher heat-transfer coefficients that can be achieved with forced circulation allow the temperature difference between heat source and sink to be minimal, thereby reducing formation of encrustations on the heat-transfer surface. The operation of cooling crystallizers is limited by the tendency of the solute to form encrustations on the cooling surface, so that the temperature of the cooling fluid and the temperature decrease of the slurry flowing through the heat exchanger may be limited. It is not uncommon to limit the decrease in magma temperature to $\sim$3–5 °C; therefore, both the circulation rate and heat-transfer surface must be large.

The feed in cooling crystallizers should be rapidly mixed with the magma so as to minimize the occurrence of regions of high supersaturation, which lead to excessive nucleation. Another factor that can lead to degradation of the CSD is

the type of pump used in the circulation loop (18,33,34). An inappropriate pump can cause attrition of the crystals through abrasion, fracture, or shear, and most commercial systems use specially designed axial-flow pumps that provide high flow rates and low heads.

If the characteristics of the system are such that the operating temperature of the crystallizer is low in comparison to the temperature of cooling water, or if there are severe problems with the formation of encrustations, direct-contact refrigeration can be used (128,129). A refrigerant is mixed with the crystallizer contents and vaporized at the magma surface. On vaporizing, the refrigerant removes sufficient heat from the magma to cool the feed and remove the heat of crystallization. The refrigerant vapor must be compressed, condensed, and recycled for the process to be economical. Moreover, the refrigerant must be insoluble in the liquor to minimize losses and product contamination.

Scale formation on the heat exchanger surfaces or at the vapor–liquid interface in the crystallizer can cause operational problems with evaporative crystallizers. Such problems can be overcome by not allowing vaporization or excessive temperatures within the exchanger and by proper introduction of the circulating magma into the crystallizer. The latter may be accomplished by introducing the magma below the surface of the magma in the crystallizer, so that all vaporization occurs from a well-mixed zone or by introducing the magma so as to induce a swirling motion that is intended to dislodge encrustations from the wall of the crystallizer at the vapor–liquid interface.

Special devices for classification of crystals may be used in some applications. Figure 26 shows a draft-tube-baffle (DTB) crystallizer designed to provide preferential removal of both fines and classified product. Feed is introduced to the fines circulation line so that nuclei resulting from feed introduction can be dissolved as the stream flows through the fines dissolution exchanger. A quiescent zone is formed between the baffle extending into the chamber and the outside wall of the crystallizer. Flow through the quiescent zone can be adjusted so that crystals below a certain size (determined by settling velocity) are removed in the fines dissolution circuit.

Another type of crystallizer is the Oslo-type unit shown in Figure 27. In units of this type, the aim is to form a supersaturated solution in the upper chamber and then relieve the supersaturation through growth in the lower chamber. The use of the downflow pipe in the crystallizer provides good mixing in the growth chamber.

6.3. Melt Crystallization. The use of a solvent can be avoided in some systems. In such cases, the system operates with heat as a separating agent, as do several processes involving crystallization from solution, but formation of crystalline material is from a melt of the crystallizing species rather than a solution (130–137).

For the following reasons, melt crystallization holds great promise in situations in which it can substitute for crystallization from solution: (*1*) Without the need to recover and maintain the purity of a solvent, processing costs are reduced substantially. (*2*) Because there is no contaminated solvent to handle, melt crystallization may be more environmentally benign. (*3*) Energy costs found in evaporative crystallization obviously would be reduced if it is possible to produce a desired solid without the need to evaporate solvent (*4*). Melt crystallization can

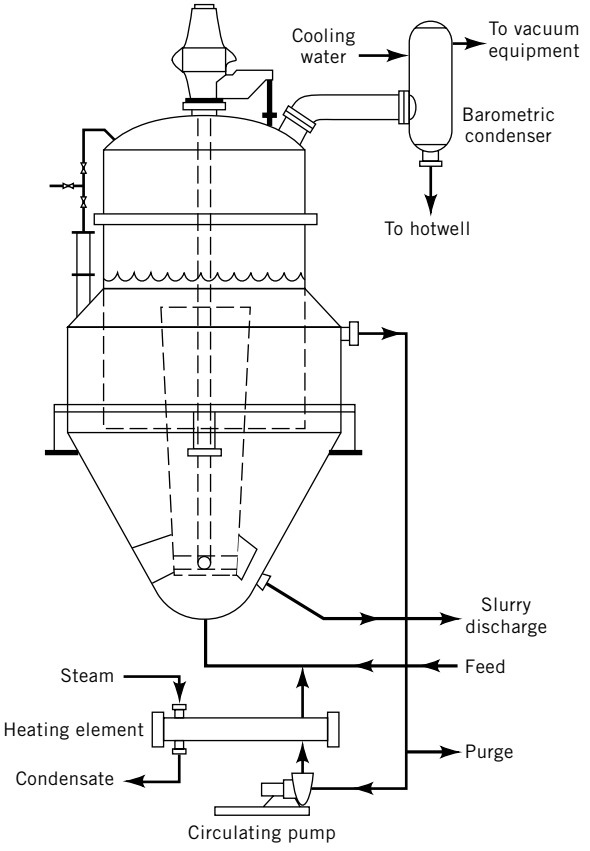

Fig. 26. Schematic diagram of DTB crystallizer.

yield high selctivities *(5)*. Melt crystallization may be a reasonable alternative to other separation and purification processes, because the heat of vaporization of most volatile organic materials is between two and five times their heat of fusion (in case of water, seven) and the temperature level is much lower than in atmospheric evaporive processes. An analysis of the energy requirements in melt processes has shown that such processes can compete with other thermal separation techniques only if the plant is well designed and the process precisely controlled (136).

Melt crystallization is carried out either with a suspension of crystals or an advancing front (layer) of solids, although a further categorization of melt crystallization is possible (130). The following is a brief review of processes in which melt crystallization is used; a more complete review, including a case study for system design, is available (125).

A suspension of crystals formed from the melt may be contacted by well-mixed mother liquor or the crystals may be moved countercurrently to liquor flow in a vertical or horizontal column. In column crystallizers, crystals are moved in a specific direction by gravity or rotating blades. The crystals are

Fig. 27. Oslo crystallizer (Messo-Oslo, Messo Chemietechnik GmbH).

melted by the addition of heat when they reach a designated end of the crystallizer; a portion of the melt is removed as product and the remainder is returned to the system to flow countercurrently (reflux) to and to wash the product crystals.

One of the early column crystallizers was that introduced for the separation of xylene isomers (see XYLENE and ETHYLBENZENE). In this unit, shown schematically in Figure 28, *p*-xylene crystals are formed in a scraped-surface chiller above the column and fed to the column. The crystals move downward countercurrently to impure liquid in the upper portion of the column and molten *p*-xylene in the lower part of the column. Impure liquor is withdrawn from an appropriate point near the top of the column of crystals while pure product, *p*-xylene, is removed from the bottom of the column. The pulse unit drives melt up the column as reflux and into a product receiver.

Many patents [like Brodie Purifier (138)] and papers [for a summary see eg, (130,131)] on suspension melt crystallization columns exist on the marked to day. Only the Kureha Chemical column (139), with a double helix screw for the

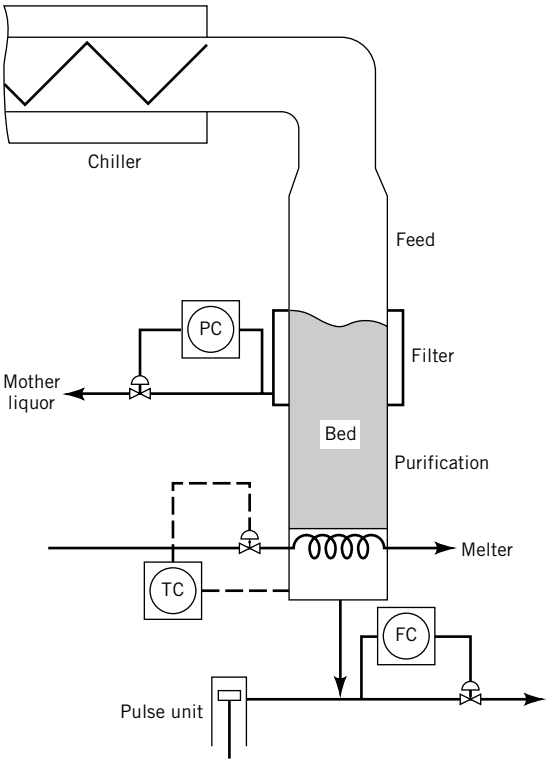

Fig. 28. Schematic diagram of a system used to separate xylene isomers (125). PC = pressure control, TC = temperature control, and FC = flow control.

crystal transport, has significant market share. In the suspension technique, however, the crystallizers with scraped-surface chillers [dewaxing of crued oil (140)] or combinations of crystallizers with so-called wash columns [dewaxing of crude oil, fruit juice concentration or wast water purification (141)] have senificant market shares.

In layer-melt crystallizations (progressive freezing), mother liquor flows over or stays in front of a cooled surface on which material is crystallized. The advancing front of crystals grows in the direction from the cooled surface into the mother liquor. A variety of techniques can be used to take advantage of this type of operation.

Figure 29 is a schematic diagram of the Sulzer-MWB process (142), which uses an operation in which there are several steps in a batch cycle. Crystal growth is on the inside of a battery of tubes through which melt is flowing, and the melt flows as a falling film. The process includes the following steps:

1. Flow of mother liquor through the cooled tubes is initiated, and crystals are grown on the tube surfaces. The heat transfer rate should be controlled so as to moderate crystal growth, thereby producing a relatively uniform layer of high purity solids.

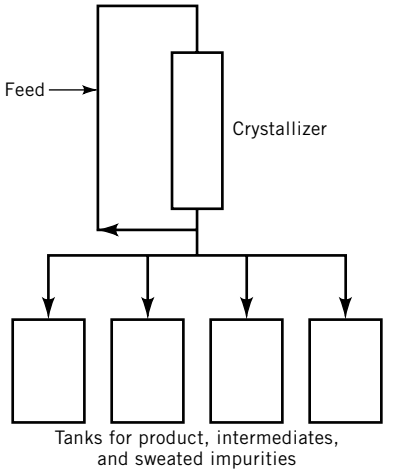

Fig. 29. Schematic diagram of the Sulzer-MWB melt crystallization process.

2. When sufficient crystal mass has been formed, melt flow is stopped and residual mother liquor is drained from the unit.
3. The solid purity is enhanced by applying heat and causing impurities to flow from the heated solids through a process known as sweating.
4. After sweating, either the cycle is returned to step 1 and additional solids are deposited or the solids present on the tube wall are melted and recovered as product.
5. The recovered product melt can be put through the cycle again to increase purity, recover product from the residue to increase the yield, or fresh feed can be introduced to the cycle.

Besides this discribed process type with forced circulation of the melt (a so-called dynamic mode) there is also a static process mode that has significant market shares. The static mode process exists as a tube type [eg, (143)] or plate type [eg, (144)], respectively.

Suspension versus solid-layer techniques exhibit the attributes outlined in Figure 30. In almost all cases, the advantage of one is the disadvantage of the other. For example, high growth rates for the solid-layer techniques (about two orders of magnitude more than in the suspension case) are made up by the low available interface for heat and mass transfer for the layer technique (about two orders of magnitude less than in the supension case).

In both techniques, product purity could be improved by postpurification processes such as sweating and washing. In general, these processes need less time, less energy than an additional crystallization step, and yield a purification effect almost as big as a crystallization step. A definition of the postpurification steps is given in Figure 31. All post purification processes are in industrial use.

FEATURE	SOLID LAYER TECHNIQUE	SUSPENSION TECHNIQUE
Apparatus	no moving parts except pumps	moving parts, especially scrapers
Operation	discontinuous (predominantly)	continuous (predominantly)
Temperature of melt	above, but close to solidification temperature	below solidification temperature
Melt flow rate	large	small
Heat withdraw	through crystal layer	through the melt
Crystal growth rates	large $10^{-5} - 10^{-7}$ m/s	small $10^{-7} - 10^{-8}$ m/s
Relative interface crystal-melt	small $10 - 10^{2}$ m^2/m^3	large 10^{4} m^2/m^3
Transportation of product	no problems, all liquid	problems due to suspensions
Solid-liquid separation	easy, just draining	difficult
Incrustation problems	no	yes
Scale-up	easy	difficult

Fig. 30. Comparison of solid layer and suspension crystallization.

The postcrystallization treatment sweating (dry sweating) is a temperature-induced purification step. After the crystallization process the temperature of the cooled surface is raised to about the melting point of the pure component. The melting takes place preferentially at the boundary of the included melt drops containing the impurities. Due to the drops' volume increase and cracks, finally, the melt is drained out of the pores and the impurities are thus expelled from the solid. This process is supported by the decrease in viscosity due to the higher temperature.

The postcrystallization treatment washing can be divided into rinsing and diffusion washing. If highly contaminated residual melt adhering to the crystal layer is substituted by a washing liquid of higher purity in a few seconds, rinsing will take place. Rinsing is a treatment driven by mechanical forces.

If the washing liquid is in contact with the front of the crystal layer for a longer period of time (~ 15 — 20 min), the impurities in liquid inclusions will diffuse out of the pores into the washing liquid in a measurable quantity. In order to avoid crystallization of the washing liquid onto the crystal layer it must be superheated. Therefore the warm washing liquid causes a sweating from the liquid side which increases the efficiency of the washing step. All three phenomena, rinsing, diffusion and sweating, are involved in the so-called diffusion washing which is a concentration driven process.

Fig. 31. All three postcrystallization steps described above for the layer technique can be and are also used in suspension crystallization processes.

BIBLIOGRAPHY

"Crystallization," in *ECT* 1st ed., Vol. 4, pp. 619–636, by A. Ralph Thompson, University of Pennsylvania; in *ECT* 2nd ed., Vol. 6, pp. 482–515, by J. W. Mullin, University of London; in *ECT* 3rd ed., Vol. 7, pp. 243–285, by J. W. Mullin, University of London; Ronald W. Rouseau, Georgia Institute of Technology in *ECT* 4th ed., Vol. 7, pp. 683–729 by Ronald W. Rouseau, George Institute of Technology; "Crystallization" in *ECT* (online), posting date: December 4, 2000, by Ronald W. Rouseau, Georgia Institute of Technology.

CITED PUBLICATIONS

1. National Research Council, *Frontiers in Chemical Engineering: Research Needs and Opportunities*, National Academy Press, Washington, D.C., 1988, Chapt. 3.

2. R. M. Felder and R. W. Rousseau, *Elementary Principles of Chemical Processes*, 2nd ed., John Wiley & Sons Inc., New York, 1986.
3. R. H. Perry and D. W. Green, eds., *Perry's Chemical Engineers' Handbook*, McGraw-Hill Book Co., Inc., New York, 1984, pp. 3–99.
4. H. Charmolue and R. W. Rousseau, *AIChE J.* **37**, 1121 (1991).
5. D. Kashehiev, *Nucleation: Basic Theory with Application*, Butterworth-Heinemann, Oxford, 2000.
6. P. Sayan and J. Ulrich, *Cryst. Res. Technol.* **36**, 411 (2001).
7. J. W. Mullin, *Crystallization*, 3 ed., Butterworth-Heinemann, Oxford, 1992.
8. H. A. Miers and F. Issac, in H. E. Buckley, *Crystal Growth*, John Wiley & Sons, Inc., New York, 1951, p. 7.
9. A. D. Randolph and M. A. Larson, *Theory of Particulate Processes*, 2nd ed., Academic Press, New York, 1988.
10. J. Garside and Roger J. Davey, *Chem. Eng. Commun.* **4**, 393 (1980).
11. M. A. Larson, *AIChE Symp. Ser.* **80**(240), 39 (1984).
12. M. W. Girolami and R. W. Rousseau, *Ind. Eng. Chem. Process Des. Dev.* **25**, 66 (1986).
13. H. Offermann and J. Ulrich, in S. J. Jancic and E. J. de Jong, eds., *Industrial Crystallization 81*, North-Holland Publishing Co., 1982, pp. 313–314.
14. C. Y. Sung, J. Estrin, and G. R. Youngquist, *AIChE J.* **19**, 957 (1973).
15. R. E. A. Mason and R. F. Strickland-Constable, *Trans. Faraday Soc.*, **62** (pt. 2), 455 (1966).
16. D. P. Lal, R. E. A. Mason, and R. F. Strickland-Constable, *J. Cryst. Growth* **5**, 1 (1969).
17. N. A. Clontz and W. L. McCabe, *Chem. Eng. Prog. Symp. Ser.* **67**(110), 6 (1971).
18. J. Ulrich, Ph.D. dissertation, RWTH-Aachen, Achen, Germany, 1981.
19. J. Ulrich and M. Kruse, *Crystal Res. Techn.* **24** 2, 181, (1989).
20. J. Ulrich and M. Kruse, in A. S. Myerson and K. Toyokura, eds., *Crystallization as a Separations Process*, American Chemical Society Symposium Series 1990, Washington D.C., pp. 43–54.
21. P. Sayan and J. Ulrich, *Cryst. Res. Technol.* **36**, 11, 1253 (2001).
22. R. W. Rousseau and W. L. McCabe, Paper presented at the World Congress on Chemical Engineering, Amsterdam, The Netherlands, June 1976.
23. R. C. Bennett, H. Fiedelman, and A. D. Randolph, *Chem. Eng. Prog.* **69**(7), 86 (1973).
24. P. A. M. Grootscholten, L. D. M. v.d. Brekel, and E. J. deJong, *Chem. Eng. Res. Des.* **62**, 179 (1984).
25. J. Garside and M. B. Shah, *Ind. Eng. Chem. Process Des. Dev.* **19**, 509 (1980).
26. M. Vendel and A. C. Rasmuson, *AIChE J.* **43** 5, 1300 (1997).
27. C. Y. Tai, W. L. McCabe, and R. W. Rousseau, *AIChE J.* **21**, 351 (1975).
28. C. Y. Tai, J.-F. Wu , and R. W. Rousseau, *J. Cryst. Growth* **116**, 294 (1992).
29. J. W. Mullin and C. L. Leci, *Phil. Mag.* **19**, 1075 (1969).
30. P. M. McMahon, K. A. Berglund, and M. A. Larson, in S. J. Jancic and E. J. deJong, eds., *Proceedings of the 9th Symposium on Industrial Crystallization*, Elsevier, Amsterdam, The Netherlands, 1984, p. 229.
31. R. M. Ginde and A. S. Myerson, *J. Cryst. Growth* **116**, 41 (1992).
32. R. J. Pohlisch, Ph.D. dissertation, TU München, Germany, 1987.
33. M. J. Gerigk, *Effektive Keimbildung in Zwangsumlauf-Kristallisatoren*, Ph.D. dissertation, RWTH Aachen, Verlag J. Mainz, Aachen, Germany, 1991.
34. C. Gahn, Ph.D. dissertation, TU München, Herbert Utz Verlag Wissenschaft, München, Germany, 1997.
35. J. Garside and N. S. Tavare, *Chem. Eng. Sci.* **36**, 863 1981.
36. M. Kruse, Ph.D. dissertation, Universität Bremen, VDI Verlag, Düsseldorf, Germany, 1993.

37. M. Kruse and J. Ulrich, in Z. H. Rojkowski, ed., *Proceedings of the 12th Symposium on Industrial Crystallization*, Warsow, Poland, Vol. 2, pp. 4- 125–4-130.
38. J. Garside, *AIChE Symp. Ser. No.* **240** 80, 23 (1984).
39. R. F. Strickland-Constable, *Kinetics and Mechanism of Crystallization*, Academic Press, New York, 1968.
40. M. Ohara and R. C. Reid, *Modeling Crystal Growth Rates from Solution*, Prentice-Hall Press, Englewood Cliffs, N.J., 1973.
41. W. K. Burton, N. Cabrera, and F. C. Frank, *Philos. Trans. R. Soc. London* **243** (A866), 299 (1951).
42. J. R. Bourne, *AIChE Symp. Ser. No.* **193** 76, 59 (1980).
43. W. L. McCabe, *Ind. Eng. Chem.* **21**, 30 (1929).
44. S. J. Jancic and P. A. M. Grootscholten, *Industrial Crystallization*, D. Reidel Publishing Com., Dordrecht, The Netherlands, 1984.
45. A. S. Myerson, *Handbook of Industrial Crystallization*, 2nd ed., Butterworth-Heinemann, New York, 2002.
46. A. Mersmann, *Crystallization Technology Handbook*, Marcel Dekker, Inc., New York, 2001.
47. S. Al-Jibbouri and J. Ulrich, *Cryst. Res. Technol.* **36**, 12, 1365 (2001).
48. E. T. White and P. G. Wright, *CEP Symp. Ser.* **67**(110), 81 (1971).
49. J. Garside and S. J. Jancic, *Chem. Eng. Sci.* **33**, 1623 (1978).
50. J. Ulrich and M. Kruse, in A. Mersmann, ed., *Proceedings of the 11th Symposium on Industrial Crystallization*, Garmisds-Portenkirchen, Germany, 1990, pp. 361–366.
51. J. Ulrich, *Crystal Res. Techn.* **24**, 3, 249 (1989).
52. A. H. Janse and E. J. de Jong, in E. J. de Jong and S. J. Jancic, eds., *Industrial Crystallization '78*, North-Holland, Amsterdam, The Netherlands, 1979, p. 135.
53. A. H. Janse and E. J. de Jong, in J. W. Mullin, ed., *Industrial Crystallization*, Plenum Press, New York, 1976, p. 145.
54. M. W. Girolami and R. W. Rousseau, *AIChE J.* **31**, 1821 (1985).
55. K. A. Berglund and M. A. Larson, *AIChE Symp. Ser. No.* **215**, 78, 9 (1982).
56. J. Ulrich, *Kristallwachstumsgeschwindigkeiten bei der Kornkristallisation – Einflu*β größen und Meβtechniken, Shaker Verlag, Reihe Verfahrenstechnik, Aachen/ Germany, 1993.
57. A. D. Randolph and E. T. White, *Chem. Eng. Sci.* **32**, 1067 (1977).
58. C. Y. Lui, H. S. Tsuei, and G. R. Youngquist, *Chem. Eng. Prog. Symp. Ser.* **67**(110), 43 (1971).
59. H. J. Human, W. J. P. van Enckevork, and P. Bennema, in J. J. Jančić and E. J. de Jong, eds., *Industrial Crystallization 81*, North Holland, Amsterdam, The Netherlands, 1982, p. 387.
60. K. A. Berglund, E. L. Kaufman, and M. A. Larson, *AIChE J.* **25**, 867 (1983).
61. K. E. Blem and K. A. Ramanarayanan, *AIChE J.* **33**, 677 (1987).
62. S. Wang, Ph.D. dissertation, TU München, Germany, 1992.
63. R. C. Zumstein and R. W. Rousseau, *AIChE J.* **33**, 121 (1987).
64. N. A. Clontz, R. T. Johnson, W. L. McCabe, and R. W. Rousseau, *Ind. Eng. Chem. Fundam.* **11**, 368 (1972).
65. J. Nyvlt and J. Ulrich, *Admixtures in Crystallization*, VCH, Weinheim, Germany, 1995.
66. S. N. Black, R. J. Davey, and M. Halcrow, *J. Cryst. Growth* **79**, 765 (1986).
67. M. Lahav and L. Leiserowitz, in A. Mersmann, ed., *Proceedings of the 11th Symposium on Industrial Crystallization*, Garmisch-Partenkirchen, Germany, 1990, p. 609.
68. S. Niehörster, Ph.D. dissertation, Universität Bremen, Der Kristallhabitus unter Additiveinfluss: Eine Modellierungs methode Papierflieger, Clausthal-Zellerfeld, Germany, 1997.

69. F. J. J. Leussen, *Rationalization of Racemate Resolution a molecular modeling study*, Ph.D. dessertation, Katholieke Universiteit Nijmegen, The Netherlands 1993.
70. R. F. P. Grimbergen, H. Meekes, and P. Bennema, eds., *Proceedings of the 4th International Workshop on Crystal Growth of Organic Materials*, Shaker Verlag, Aachen, 1997, pp. 13–24.
71. A. S. Myerson, *Molecular Modeling Applications in Crystalization*, Cambridge University Press, Cambridge, U.K., 1999.
72. R. M. Geertman, Ph.D. dissertation, Katholieke Universiteit Nijmegen, The Netherlands 1996.
73. C. S. Strom and P. Bennema, in J. Ulrich,, ed., *Proceedings of the 4th International Workshop on Crystal Growth of Organic Materials*, Shaker Verlag, Aachen, Germany, 1997, pp. 85–93.
74. L. Addadi, Z. Berkovitch-Yellin, N. Domb, E. Gati, M. Lahav, and L. Leiserowitz, *Natur. (London)* **296**(4), 21 (1982).
75. S. Niehörster, J. Ulrich, *Crystal Res. Technol.* **30**(3), 391 (1995).
76. J. D. H. Donnay and D. Harker, *Am. Mineral* **22**, 446 (1937),
77. P. Hartman and W. G. Perdok, *Acta Crystallo.* **8**, 521 (1955).
78. P. Hartman and Bennema, *J. Cryst. Growth* **49**, 145 and 157 (1980).
79. B. D. Chen, J. Garside, R. J. Davey, S. J. Maginn, and M. Matsuoka, *J. Phys. Chem.* **98**, 3215 (1994).
80. M. Mattos, Ph.D. dissertation, Universität Bremen, Shaker Verlag, Aachen, Germany, 1999.
81. E. P. G. van den Berg, *Morphology*, Ph.D. dissertation Katholieke Universiteit Nijmegen), Katholieke Universiteit Nijmegen, Nijmegen, The Netherlands 1997.
82. S. Nordhoff, R. Dümpelmann, G. Wagner, and J. Ulrich, in J. Ulrich, ed., *Proceedings of the 4th International Workshop on Crystal Growth of Organic Materials*, Shaker Verlag, Aachen, Germany, 1997, pp. 325–332.
83. G. Henning, in Ref. 67, p. 113.
84. M. J. Hounslow, R. L. Ryall, and V. R. Marshall, *AIChE J.* **34**, 1821 (1988).
85. P. Marchal, R. David, J. P. Klein, and J. Villermaux, *Chem. Eng. Sci.* **43**, 59 (1988).
86. R. C. Zumstein and R. W. Rousseau, *Chem. Eng. Sci.* **44**, 2149 (1989).
87. M. W. Girolami and R. W. Rousseau, *J. Cryst. Growth* **71**, 220 (1985).
88. N. Hiquily and C. Laguérie, in S. J. Jancic and E. J. deJong, eds., *Industrial Crystallization '84*, Elsevier, Amsterdam, The Netherlands, 1984, p. 79.
89. M. Poschmann, Ph.D. dissertation Universität Bremen, Shaker Verlag, Aachen, Germany, 1995.
90. M. Matsuoka, M. Ohishi, and Sh. Kasama, *J. Chem. Eng. Jpn.* **19**, 3, 181 (1986).
91. S. N. Black and R. J. Davey, *J. Cryst. Growth* **90**, 136 (1988).
92. K. G. Denbigh and E. T. White, *Chem. Eng. Sci.* **21**, 739 (1966).
93. N. Kubota, N. Doki, A. Sato, M. Yokota, O. Hamada, and F. Masumi, *Proceedings of International Symposium on Industrial Crystallization*, PR China, 1998, Chemical Industry Press, pp. 26–30.
94. A. S. Myerson and D. J. Kirwan, *Ind. Eng. Chem. Fundam.* **4**, 414 (1977).
95. A. S. Myerson and D. J. Kirwan, *Ind. Eng. Chem. Fundam.* **4**, 420 (1977).
96. N. Hiquily, C. Laguérie, and J. P. Couderc, *Chem. Eng. J.* **30**, 1 (1985).
97. S. Henning, S. Niehörster, and J. Ulrich, in A. S. Myerson, D. A. Green, and P. Meenan, eds., *Crystal Growth of Organic Materials*, American Chemical Society, Symposium Series. 1996, Washington, D. C., pp. 163–171.
98. S. Henning and J. Ulrich, *Trans I ChemE*, 75, Part A **2**, 233 (1997).
99. S. Henning and J. Ulrich, in J. Ulrich,, ed., *Proceedings of the 4th International Workshop on Crystal Growth of Organic Materials*, Shaker Verlag, Aachen, Germany, 1997, pp. 269–276.

100. K.-J. Kim and J. Ulrich, *J. Phys. D: Appl. Phys.* **34**, 1308 (2001).
101. D. H. Jenkins and H. N. Sinha, in Ref. 51.
102. R. C. Zumstein, T. Gambrel, and R. W. Rousseau, in A. S. Myerson and K. Toyokura, eds., *Crystallization as a Separations Process*, ACS Symposium Series. No. 438, 1990, Washington, D.C., p. 85.
103. R. C. Zumstein and R. W. Rousseau, *AIChE Symp. Ser.* **83**(253), 130 (1987).
104. R. W. Rousseau and R. M. Parks, *Ind. Eng. Chem. Fundam*. **20**, 71 (1981).
105. J. R. Beckman and A. D. Randolph, *AIChE J.* **23**, 510 (1977).
106. R. W. Rousseau and T. R. Howell, *Ind. Eng. Chem. Process Des. Dev.* **21**, 606 (1982).
107. S. Heffels and M. Kind, *Proceedings of the 14th International Symposium on Industrial Crystallization*, Cambridge, U.K., Institution of Chemical Engineers, 1999, p. 51.
108. W. Beckmann, W. Otto, and U. Budde, *Crystallization of the Stable Polymorph of Hydroxytriendione: Seeding Process and Effects of Purity*, Organic Process Research & Development A.
109. M. Parisi and A. Chianese, *Proceedings of the 8th International Workshop on Industrial Crystallization*, (Biwid) Doc Vision Delft, The Netherlands, 2001, pp. 126–133.
110. N. S. Tavare, *Industrial Crystallization: process simulation analysis and design*, Plenum Press, New York, London, 1994.
111. W. Omar and J. Urich, *Cryst. Res. Technol.* **34**(3), 379 (1999).
112. W. Omar and J. Ulrich, *Proceedings of the 14th International Symposium on Industrial Crystallization Cambridge, U.K., IChem^E*, 1999, p. 159.
113. C. Strege, W. Omar, and J. Ulrich, in J. Ulrich,, ed., *Proceedings of the 7th International Workshop on Industrial Crystallization*, (Biwid), Mortin-Luther-Universität Halle-Wittenberg, Halle, Germany 1999, pp. 219–230.
114. M. S. Uusi-Penttilä, K. A. Berglund, in J. Ulrich,, ed., *Proceedings of the 4th International Workshop on Crystal Growth of Organic Materials*, Shaker Verlag, Aachen, Germany, 1997, pp. 245–252.
115. N. S. Tavare, J. Garside, and M. R. Chivate, *Ind. Eng. Chem. Process Des. Dev.* **19**, 653 (1980).
116. A. G. Jones, A. Chianese, and J. W. Mullin, in Ref. 51.
117. G. L. Zipp and A. D. Randolph, in J. Nývlt and S. Zacek, eds., *Proceedings of the 10th Symposium on Industrial Crystallization*, Elsevier, New York, 1989, p. 469.
118. B. Bechtloff, P. Jüsten, J. Ulrich, *Chem. Ingenieur Tech.* **73**(5), 453 (2001).
119. J. Garside, R. J. Davey, and A. G. Jones, *Advances in Industrial Crystallization*, Butterworth-Heinemann, Oxford, 1991.
120. E. M. Berends, *Supercritical Crystallization: The Ress-Process and the Gas-Process*, Ph.D. dissertation, TU Delft, The Netherlands, 1994.
121. T. G. Zijlema, *The Antisolvent Crystallization of Sodium Chloride*, Ph.D. dissertation, TU Delft, The Netherlands, 1999.
122. H. Weber, Ph.D. dissertation, Universität Bremen, Shaker Verlag, Aachen, Germany, 1999.
123. H. Kröber, U. Teipel, and H. Krause, *Proceedings of the 14th International Symposium on Industrial Crystallization IChem^E*, Cambridge, U.K., 1999, p. 43.
124. R. Bennett in Ref. 3, Chapt. 19.
125. R. W. Rousseau and C. G. Moyers in R. W. Rousseau, ed., *Handbook of Separation Process Technology*, John Wiley & Sons, Inc., New York, 1987, Chapt. 11.
126. G. Hofmann, in J. P. van der Eerden and O. S. L. Bruinsma, *Science and Technology of Crystal Growth*, Kluwer Academic Publishers, Dordrecht, Boston, London, 1995, pp. 221–232
127. W. Wöhlk and G. Hofmann, *Int. Chem. Eng.* **27**(2), 197 1987.

128. K. Bartosch and A. Mersmann, *Proceedings of the 14th International Symposium on Industrial Crystallization IChem^E*, Cambridge, U.K., 1999, p. 49.
129. K.-J. Kim and A. Mersmann, *Proceedings of the 13th Symposium on Industrial Crystallization IChem^E*, Cambridge, U.K., 1996, pp. 176–182.
130. J. Ulrich, in A. S. Myerson, ed., *Handbook of Industrial Crystallization*, 2nd ed., Butterworth-Heinemann, Oxford, 2002, pp. 161–179.
131. J. Ulrich, J. Bierwirth, and S. Henning, *Separation and Purification Methods* **25**, 1, 1 (1996).
132. M. Y. Özoguz, Ph.D. dissertation, Universität Bremen, VDI-Verlag, Düsseldorf, Germany, 1992.
133. P. J. Jansens and G. M.. van Rosmalen, in D. J. T. Hurle, ed., *Handbook of Crystal Growth*, Vol. 2A, Elsevier Science Publishers, Amsterdam, The Netherlands, 1994, Chapt. 6.
134. G. F. Arkenbout, *Melt Crystallization Techology*, Technomic Publishing Company, Inc., Lancaster, Penn., 1995.
135. M. Matsuoka, in J. Garside, R. J. Davey, and A. G. Jones, eds., *Advances in Industrial Crystallization*, Butterworth-Heinemann, Oxford, 1991, pp. 229–244.
136. G. J. Sloan and A. R. McGhie, *Techniques of Melt Crystallization*, John Wiley & Sons, New York, 1988.
137. K. Toyokura, I. Hirasawa, K. Wintermantel, and G. Wellinghoff, in A. Mersmann, ed., *Crystallization Technology Handbook*, Marcel Dekker, Inc., New York, Basel, 2001, pp. 617–702.
138. J. A. Brodie, *Mech. Chem. Eng. Trans. Inst. Eng.* **7**(1), 37 (1971).
139. J. Yamada, C. Shimizu, and S. Saitoh, in S. J. Jancic and E. J. de Jong, eds., *Industrial Crystallization* 81, North-Holland Publishing Co., 1981, pp. 265–270.
140. A. J. Armstrong, *Br. Chem. Eng.* **14**, 647 (1969).
141. R. Scholz, R. Rümekorf, R. Wagner, S. Nordhoff, and M. Creutz, *Proceedings of the 8th International Workshop on Industrial Crystallization*, DocVision Delft, The Netherlands, 2001, pp. 8–17.
142. M. Stepanski and U. Haller, *Hydrocarbon Eng.* **4**, 33 (2000).
143. U.S. Pat. 3,597,164 (1968) C. Ab-Der-Halden.
144. M. Stepanski, *Proceedings of the 14th International Symposium on Industrial Crystallization*, Institution of Chemical Engineers, Cambridge, U.K., 1999, p. 5.

JOACHIM ULRICH
Martin-Luther-University